Chapter 8—Reanalysis of the Alkoxy k_{isom}/k_{O2} OH-stretch Experiment and a New Interpretation of Alkoxy Relative Kinetics Experiments

Abstract

In Chapter 7, we showed that the ν_1 band of the primary products of alkoxy isomerization could be used to measure the relative rate of isomerization to reaction with O_2 (k_{isom}/k_{O2}). Previous studies within the Okumura group measured the relative kinetics of *n*-butoxy and 2-pentoxy via the ν_1 band, obtaining k_{isom}/k_{O2} values with low uncertainties, but generally higher than those reported in the literature. We find that the cause of this discrepancy is multiple errors in the analysis of the relative kinetics data. Amongst these errors were the calculations of [RONO], [O_2], photolysis flux, and relative absorbance (A_0/A), due to errors in the CRDS program or errors in scaling data to [RONO]. Additionally, the effects of additional alkoxy reactions (decomposition, reaction with NO, prompt decomposition, and prompt isomerization) were not considered. A full reanalysis of all data (gas flows, [RONO] monitoring, CRDS absorption data, inclusion of all reaction pathways) gives new values of **k_{isom}/k_{O2} of (1.69±0.15) × 10^{19} cm^{-3} for *n*-butoxy, and (3.37 ± 0.43) × 10^{19} cm^{-3} for 2-pentoxy (2σ error)**. The *n*-butoxy value of k_{isom}/k_{O2} is in much better agreement with the rest of the literature, but with a significantly smaller uncertainty than previous studies. The reanalyzed data give an estimate of ϕ_{pi} (the fraction of alkoxy radicals that undergo prompt isomerization following photolysis of alkyl nitrite at 351 nm) as 0.04 ± 0.02 for *n*-butoxy and 0.05 ± 0.02 for 2-pentoxy. We show that the previous experiments detected a mixture of primary and secondary products, although the results of Chapter 7 suggest that this does not affect the value of k_{isom}/k_{O2} obtained from our data.

Introduction

In Chapter 7, we showed that CRDS is capable of detecting the primary products of alkoxy isomerization, HOR• (in the absence of oxygen) and HOROO• (in the presence of oxygen), by measurement of the ν_1 (OH stretch) vibrational spectrum. We have also shown that this band can be used to measure the relative rate constant of alkoxy isomerization to reaction with O_2 (k_{isom}/k_{O2}) for two reasons. First, the band intensity decreases with increasing [O_2], in agreement with our expectations for the alkoxy system. Second, the ν_1 band shape and intensity of HOROO• remain constant for at least 800 μs after reaching its maximum absorbance, making the ν_1 band a robust measure of [HOROO•].

In 2006, Mollner[30] (assisted by me in the laboratory) used the ν_1 bands of δ-HOC_4H_8•, δ-HOC_4H_8OO•, δ-HO-1-C_5H_{10}•, and δ-HO-1-$C_5H_{10}OO$• to determine k_{isom}/k_{O2} for *n*-butoxy and 2-pentoxy. Mollner's relative kinetics data sets consisted of many more data points (177 for *n*-butoxy, 95 for 2-pentoxy) than the data presented in Chapter 7 (12 for *n*-butoxy, 7 for 2-pentoxy). Mollner's relative kinetics data are shown are Figure 8.1, and k_{isom}/k_{O2} values are compared to the chemical literature in Table 8.1. We immediately note that Mollner's *n*-butoxy value is larger than the rest of the measurements. Although Mollner's measurement is within the uncertainty of the end-product studies, it is in disagreement with the measurements reported from our alkoxy studies using the ν_1 (Chapter 7) and A-X bands (Chapter 10). Comparison of the 2-pentoxy values is a challenge because of the large errors associated with each k_{isom}/k_{O2}.

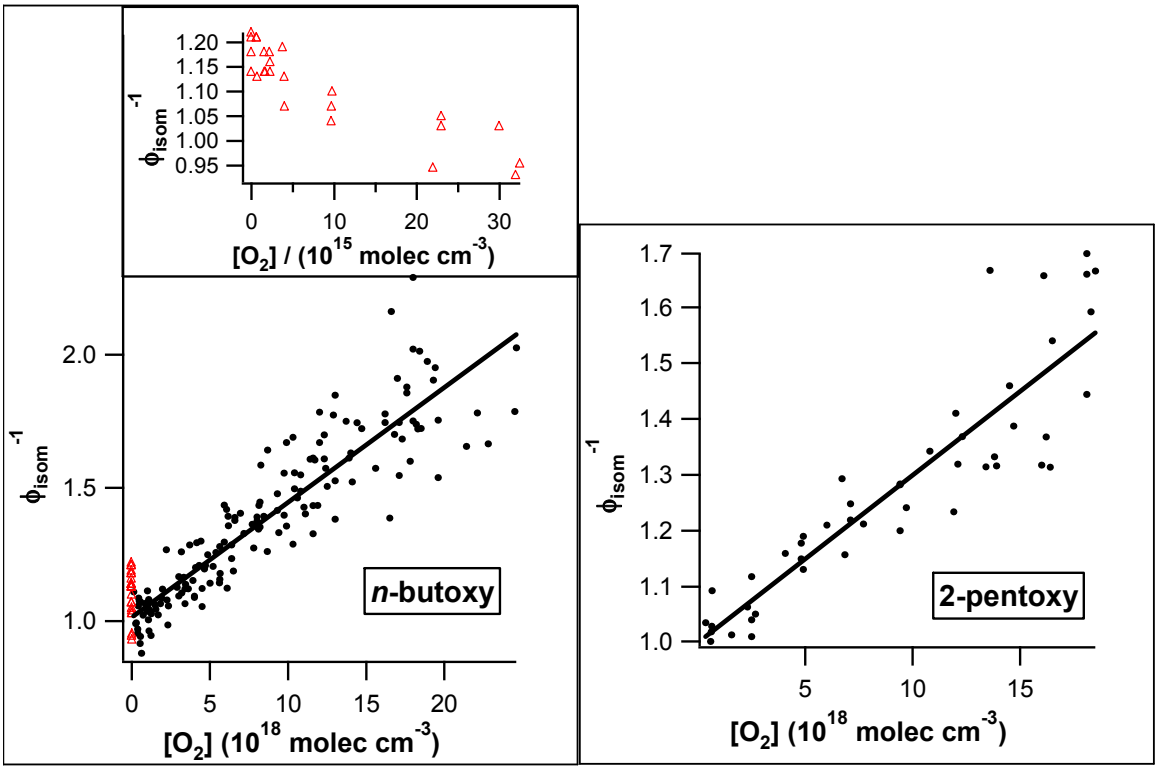

Figure 8.1. (caption and figure adapted from Mollner)[30] A_0/A (labeled as ϕ_{isom}^{-1}) plotted as a function of $[O_2]$ for n-butoxy (left) and 2-pentoxy (right). [HOR•], the concentration of all products formed through the isomerization channel, was calculated from the strength of the OH-stretch infrared peak. [RO•] was determined from the linear regression of individual data sets, assuming $\phi_{isom} = 1$ at $[O_2] = 0$. Both plots show the expected decrease in [HOR•]/[RO•] with $[O_2]$. The inset to the n-butoxy plot shows an apparent increase in $[HOC_4H_8•]$ with $[O_2]$ at very low $[O_2]$, as discussed in Chapter 9. Only the data with $[O_2] > 5 \times 10^{16}$ molecules cm^{-3} were used in the linear fits to determine k_{isom}/k_{O2}. *n*-butoxy: slope = $(4.3 \pm 0.2) \times 10^{-20}$ cm^3, intercept = 1.01 ± 0.02, $k_{isom}/k_{O2} = (2.3\ [+0.2, -0.3]) \times 10^{19}$ cm^{-3}. 2-pentoxy: slope = $(3.0 \pm 0.3) \times 10^{-20}$ cm^3, intercept = 1.00 ± 0.04, $k_{isom}/k_{O2} = (3.3\ [+0.4, -0.6]) \times 10^{19}$ cm^{-3}. All errors are reported to 2σ, asymmetric error due to prompt isomerization.

Table 8.1. Comparison of relative rate constant determinations k_{isom}/k_{O2} and derived k_{isom} for *n*-butoxy using our initial analysis of CRDS data[30]

	k_{isom}/k_{O2} (10^{19} cm^{-3})[a]	k_{isom} (10^5 s^{-1})[b]	Molecules detected	Method	*P* *(torr)*	Ref
***n*-butoxy**	**2.3 (+0.2, −0.3)**	**3.2 ± 1.6**	**δ-hydroxy-*n*-butyl peroxy**	**Slow flow, CRDS (OH Str)**	**670**	**Mollner[30]**
	1.96 ± 0.25	2.7 ± 1.4	δ-hydroxy-*n*-butyl peroxy	Slow flow, CRDS (OH Str)	330	Chapter 7
	1.39 ± 0.47	2.0 ± 1.2	δ-hydroxy-*n*-butyl peroxy	Slow flow, CRDS (A-X)	330	Chapter 10
	2.0 ± 0.4	2.7 ± 1.5	Butyl nitrite, Butanal,	Static, FTIR	700	Cassanelli[155]
	1.5 ± 0.4	2.1 ± 1.2	4-hydroxy butanal	Static, GC	760	Cox[156]
	1.9 ± 0.4	2.7 ± 1.4	Butane, Butanal	Static, FTIR	700	Niki[148]
	2.1 ± 0.5	2.9 ± 1.6	Butyl nitrite, Butanal	Slow flow, GC	760	Cassanelli[160]
	1.8 ± 1.1	2.5 ± 2.0	Butyl nitrite, Butanal	Slow flow, GC	760	Cassanelli[160]
	1.8 ± 0.6	2.5 ± 1.5	Butane, Butanal	Static, FTIR	760	Geiger[161]
	0.25 ± 0.19[c]	0.35 ± 0.20[c]	Butanal, 4-hydroxy butanal	Fast flow, LIF	38	Hein[159]
	1.6	2.2	OH and NO_2	Static, GC	740	Carter[154]
	2.1 ± 1.8[d]	2.9 ± 1.4[d]		Recommendation	760	IUPAC[118]
2-pentoxy	**3.3 (+0.4, −0.6)**	**2.7**	**δ-hydroxy-*n*-pentyl peroxy**	**Slow flow, CRDS (OH Str)**	**670**	**Mollner[30]**
	3.78 ± 1.62	3.0	δ-hydroxy-*n*-pentyl peroxy	Slow flow, CRDS (OH Str)	330	Chapter 7
	3.1[e]	2.5[e]	2-pentanone	Static, GC	700	Atkinson[145]
	0.15	0.12[f]	Acetone, Acetaldehyde, 2-hexanol	Static, GC	760	Dóbé[157]

a) All uncertainties are 2σ. All studies other than the current work treat all alkoxy reactions besides isomerization and reaction with O_2 as negligible.
b) Computed k_{isom} assuming literature value of $k_{O2} = (1.4 \pm 0.7) \times 10^{-14}$ cm^3 s^{-1} for *n*-butoxy,[28] and $k_{O2} = 8 \times 10^{-15}$ cm^3 s^{-1} for 2-pentoxy (no estimate available for the uncertainty).[142]
c) Unlike the other studies, Hein directly measured k_{isom}. In this table, we calculate the ratio k_{isom}/k_{O2} from Hein's measurement using the literature value of k_{O2}.
d) The IUPAC recommendation for k_{isom}/k_{O2} is computed from their individual recommendations of the isomerization and O_2 reactions
e) The uncertainty on k_{isom}/k_{O2} is reported by Atkinson as a factor of 2.
f) Dóbé's study calculates k_{isom} from the relative rate k_{isom}/k_{decomp} and their measured rate $k_{decomp} = 1.2 \times 10^4$ s^{-1}. The k_{isom}/k_{O2} reported in this table uses the literature value of $k_{O2} = 8 \times 10^{-15}$ cm^3 s^{-1} for 2-pentoxy.[142]

Because Mollner's and my CRDS experiments for *n*-butoxy are in disagreement, I wanted to take another look at the OH-stretch data to make sure that nothing was wrong with the data. My expectation was that nothing would be wrong, and that the discrepancies could be explained by the lack of data points in my ν_1 (Chapter 7) and A-X (Chapter 10) relative kinetics data.

As I reviewed our lab notebook, I saw some disturbing notes. One entry noted that for a pressure of 700 torr, the concentration of O_2 in the cell was 2.46×10^{19} cm^{-3}. In other words, the cell had a total pressure of 700 torr, with $[O_2]$ = 760 torr, a physical impossibility. A manual calculation of $[O_2]$ using the recorded flowmeter voltages and calibrations gave a value of $[O_2]$ approximately 10% lower than the recorded value. A check of other entries in the lab notebook between March 2006 to October 2006 revealed the same problem throughout. The problem was an error in the LabVIEW program controlling the CRDS apparatus. A single flow was subtracted out of the total gas concentration, which happened to be the right purge flow (kept roughly at 10%). The protocol in the IR-CRDS lab since March 2006 (and likely far beyond then) was to blindly copy $[O_2]$ reported by the program. **The result is that all $[O_2]$ recorded for the alkoxy experiment are 7%–10% too high, directly affecting the reported k_{isom}/k_{O2} values that we report.** This issue prompted the full reanalysis of the alkoxy data.

As I performed the reanalysis of the alkoxy data, I noticed other errors in the analysis of the alkoxy data. First, **in some of the experiments, incorrect flowmeter calibrations were entered, causing additional errors in the derived gas concentrations.** At one point, zero-flow offsets for N_2 were entered into the computer, despite Ar being sent through the flowmeters. The result was major errors in the calculation of gas concentrations.

Second, [RONO] was not calculated correctly, a major problem because the measured absorptions must be scaled to the amount of alkyl nitrite before converting absorptions to A/A_0. [RONO] in the CRDS cell is affected by the gas flow calculation problems mentions above. Three methods can be used to obtain [RONO]:

1. Measurement of [RONO] in the RONO gas line using its UV absorption at 254 nm, then calculating its dilution in the CRDS cell based on the gas flows
2. Calculating [RONO] at the bubbler using thermodynamic properties (enthalpy of vaporization and boiling point), then calculating its dilution in the CRDS cell based on the gas flows
3. Measuring the background ringdown time in the CRDS experiment, since RONO has a broad absorption in the 3500-3700 cm^{-1} range where we are measuring the alkoxy isomerization product

We only scaled to [RONO] using method 3 during our previous experiments. Worse yet, we scaled our data to $1/\tau$, the absolute background ringdown time. This is an incorrect scaling method because the vacuum ringdown time, $1/\tau_0$, was not subtracted out. **Thus, we did not actually scale to the RONO absorption.** Furthermore, since any of the three methods are equally valid for scaling, we should have checked all three to see which one gives the best fit for each individual data set.

Third, the photolysis flux was likely calculated incorrectly for these experiments, resulting in the fraction of RONO that is photolyzed being incorrectly calculated. The amount of RONO that is photolyzed can be calculated from Equation 8.1:

$$\%_{photolysis} = \frac{\left(P_{excimer} \middle/ A_{meter}\right)}{F_{excimer}} \left(\frac{\lambda}{hc}\right) \left(\sigma_{RONO,\lambda}\right) (X) \left(\frac{A_{UV,laser}}{A_{UV,CRDS}}\right), \tag{8.1}$$

where $\%_{photolysis}$ is the fraction of RONO that is photolyzed, ($P_{excimer}/A_{meter}$) is the power meter reading directly out of the excimer laser (the power meter has a 1 cm^2 area), $F_{excimer}$ is the repetition rate of excimer (10 Hz), h is Planck's constant, c is the speed of light, λ is the wavelength of the excimer light (351 nm), $\sigma_{RONO,\lambda}$ is the absorption cross section of

RONO at the excimer wavelength (8×10^{-20} cm^2 molec^{-1}), X is the quantum yield for photolysis (taken to be 1), $A_{UV,laser}$ is the area of excimer beam measured at the excimer laser output, and $A_{UV,CRDS}$ is the area of excimer beam measured at the CRDS cell.

At some point in the past, the excimer beam area at the CRDS cell was the same as the beam area directly out of the laser. Therefore, in the calculation of flux, the ratio of excimer beam areas will cancel out of the equation. However, this does not hold true when the beam areas are different, as has been true for all of the experiments in our laboratory since (and including) alkoxy. For the alkoxy experiments, $A_{UV,laser}/A_{UV,CRDS}$ = 2.5, a factor that was accounted for in some of the early experiments, and not accounted for in other experiments. **The result is that [RO•] is inconsistently calculated. However, if the photolysis flux is kept constant for a set of relative kinetics data, then we will be insensitive to this mistake since k_{isom}/k_{O2} is derived from relative absorbance measurement: absolute [RO•] is largely irrelevant.**

Additionally, the relative absorbance A_0/A was calculated in a very sloppy fashion. Rather than scale each regression line such that the y-intercepts were equal to 1, the previous analysis made use of the [RONO] measurements to scale all of the measured absorptions to [RO•] to 2×10^{14} cm^{-3}. However, this is not a good way to calculate relative absorbances, because this method requires good knowledge of [RONO] and [RO•]. Given the variations in excimer flux and the incorrect scaling to [RONO], we cannot claim to know either concentration to very good precision. **The result is that our reported absorbance data are possibly incorrect, leading to even further scatter in our plot of relative absorbance vs [O_2], and added uncertainty in the derived k_{isom}/k_{O2}.**

Finally, our previous interpretation of the alkoxy relative kinetics data ignored the effects of additional alkoxy reaction pathways. Alkoxy radicals in our experiments are generated from photolysis of an alkyl nitrite (RONO). The resulting alkoxy radicals that are formed are either in the vibrational ground state (denoted RO•, Reaction 8.2), or are vibrationally hot (denoted [RO•]*, Reaction 8.3). Once formed, the ground state alkoxy radicals can isomerize and associate with O_2 (Reaction 8.4), react with O_2 (Reaction 8.5), decompose (Reaction 8.6), or recombine with NO (Reaction 8.7). The hot alkoxy radicals can promptly isomerize (Reaction 8.8) or promptly decompose (Reaction 8.9), without regard for the thermal rate constants.

$$\mathrm{RONO} \xrightarrow{h\nu} \mathrm{RO\bullet} + \mathrm{NO} \tag{8.2}$$

$$\mathrm{RONO} \xrightarrow{h\nu} \left[\mathrm{RO\bullet}\right]^{*} + \left[\mathrm{NO}\right]^{*} \tag{8.3}$$

$$\mathrm{RO\bullet} \xrightarrow{\text{isom}} \mathrm{HOR\bullet} \xrightarrow{+O_2} \mathrm{HOROO\bullet} \tag{8.4}$$

$$\mathrm{RO\bullet} + \mathrm{O_2} \longrightarrow \mathrm{R'CHO} + \mathrm{HO_2} \tag{8.5}$$

$$\mathrm{RO\bullet} \longrightarrow \mathrm{HCHO} + \mathrm{R''\bullet} \tag{8.6}$$

$$\mathrm{RO\bullet} + \mathrm{NO} \longrightarrow \mathrm{RONO} \tag{8.7}$$

$$\left[\mathrm{RO\bullet}\right]^{*} \xrightarrow{\text{prompt isom}} \mathrm{HOR\bullet} \xrightarrow{+O_2} \mathrm{HOROO\bullet} \tag{8.8}$$

$$\left[\mathrm{RO\bullet}\right]^{*} \xrightarrow{\text{prompt decomp}} \mathrm{HCHO} + \mathrm{R''\bullet} \tag{8.9}$$

The typical analysis found in the literature considers only Reactions 8.4 and 8.5 relevant to alkoxy relative kinetics measurements; Reactions 8.6–8.9 are assumed to be negligible.[146, 148, 153-158] However, there is evidence in the literature that this is an invalid assumption. First, the recombination of alkoxy radicals with NO is fast, with a rate constant $k_{NO} = 3.32 \times 10^{-11}$ cm^3 s^{-1}.[32] For [NO] = (1–9) × 10^{14} molec cm^{-3} (typical values

of [NO] in alkoxy experiments),[146, 148, 153-158] the relative rate of NO recombination to isomerization is $\frac{k_{NO}[\mathrm{NO}]}{k_{isom}} = 0.01 - 0.12$. Second, while decomposition is slow for *n*-butoxy ($k_{\mathrm{decomp}} = 600\ \mathrm{s}^{-1}$, $k_{\mathrm{decomp}}/k_{\mathrm{isom}} = 2.4 \times 10^{-3}$), decomposition is non-negligible for 2-pentoxy, with theoretical estimates of $k_{\mathrm{decomp}} = (0.5\text{–}3) \times 10^{4}\ \mathrm{s}^{-1}$,[117] and one experimental study obtaining $1.1 \times 10^{4}\ \mathrm{s}^{-1}$.[157] For these decomposition rates, $k_{\mathrm{decomp}}/k_{\mathrm{isom}} = 0.02\text{–}0.12$.

Prompt processes may also be important (Reactions 8.8 and 8.9). The enthalpy of breaking the O-NO bond in *n*-butyl nitrite is 40 kcal mol^{-1}.[186] Photolysis using 351 nm light provides 80 kcal mol^{-1} of energy, resulting in 40 kcal mol^{-1} of excess energy distributed between the alkoxy radical and NO. Previous experiments have already estimated 10% prompt decomposition of *n*-butoxy following photolysis of *n*-butyl nitrite at 370 ± 10 nm.[155] Furthermore, theoretical calculations have shown isomerization to have a barrier of only 10 kcal mol^{-1}.[136-138] Therefore, some of the alkoxy radicals formed may isomerize immediately upon formation, without regard as to whether or not other reaction channels exist. These isomerization products are not indicative of the competition between isomerization and reaction with O_2, and thus will affect spectroscopic measurements of $k_{\mathrm{isom}}/k_{\mathrm{O2}}$.

Reactions 8.6–8.9 will consume alkoxy radicals, and therefore change the dependence of [HOROO•] on [O_2]. Since the magnitude of each reaction is on the same order of magnitude of our uncertainty for $k_{\mathrm{isom}}/k_{\mathrm{O2}}$ (10%), we cannot ignore these reactions in our analysis of our alkoxy relative kinetics data.

To summarize, the six errors in the previous alkoxy relative kinetics analysis were incorrect calculation of [O_2], incorrect computation of gas flows, incorrect scaling of data

to [RONO], incorrect calculation of photolysis flux, incorrect calculation of A_0/A, and ignoring the additional reactions of RO•. These six errors affect nearly all of the required analysis of the alkoxy data set. **Therefore, a full reanalysis of our CRDS alkoxy data must be performed.**

This thesis chapter describes the reanalysis and new interpretation of our previous alkoxy relative kinetics experiments. Gas flows and concentrations, alkoxy concentrations, scaling factors, and linear regressions were recalculated to correct the errors described above. We then derive the dependence of our CRDS absorbances on $[O_2]$, and how k_{isom}/k_{O2} can be extracted from our data.

Methods

A full description of the methods and equations used to reanalyze the alkoxy data can be found below. Briefly, reanalysis of the alkoxy data sets required five calculations:

1. Recalculation of all gas concentrations for each scan (and therefore $[O_2]$) based on the CRDS cell pressure, flowmeter voltages, zero flow offsets, and flowmeter calibrations recorded in the laboratory notebook
2. Recalculation of absolute [RONO] and [RO•] based on excimer flux, 254 nm absorption measurements, and the thermodynamic properties of the alkyl nitrites. Also, recalculation of relative [RONO] for each data set based on the background $1/\tau$-$1/\tau_0$ at the peak OH stretch wavelength.
3. Rescaling of alkoxy absorptions to the three recalculated [RONO] in order to obtain correctly scaled A_0/A (absorbance at $[O_2] = 0$ relative to measured absorbance)

4. Choosing the best fits from each data set to obtain an overall data set of A_0/A
5. Derivation of the dependence of A_0/A on $[O_2]$ to determine how to extract k_{isom}/k_{O2} from our data.

The resulting data sets were then used in our new analysis of the relative kinetics in order to extract k_{isom}/k_{O2}. This analysis also allowed us to determine the fraction of prompt isomerization.

Recalculation of Gas Concentrations

The gas flow through a mass flowmeter can be calculated from Equation 8.10:

$$f = (V - V_0)(calib), \tag{8.10}$$

where f is the gas flow (in sccm), V is the voltage across the mass flowmeter for flow f (measured by a digital readout box), V_0 is the voltage across the mass flowmeter for zero gas flow (the zero flow offset), and *calib* is the flowmeter's calibration factor (in sccm/volt). The calibration factor depends on the type of gas being used, and must be updated when gases are changed. The zero flow offset fluctuates from day to day and also depends on the type of gas being used.

Once all of the individual gas flows have been calculated, the concentrations of each gas can be computed from Equation 8.11:

$$[\text{gas}]_i = \frac{f_i}{\sum f_i}(p)\left(3.24\times10^{16}\ \frac{\text{molec}/\text{cm}^3}{\text{Torr}}\right), \tag{8.11}$$

where $[\text{gas}]_i$ is the concentration of the gas from flow i in molec cm^{-3}, f_i is the flow of interest, $\sum f_i$ is the sum of all gas flows, and p is the pressure of the CRDS cell in torr. If

the gas of interest is on multiple gas lines, all of those lines must be added together to obtain the total concentration.

Recalculation of [RONO] and [RO•]

It is possible to obtain absolute [RONO] and [RO•] through two methods and relative [RONO] and [RO•] through a third method. The first method to obtain [RONO] makes use of the UV absorption of RONO at 254 nm. The absorption cross section for C_4H_9ONO is $\sigma_{RONO,254nm} = 1.3 \times 10^{-18}$ cm^{-2},[32, 192] and our quantum chemistry calculations (CIS/6-31+G(d,p)) suggest that the cross section of 2-$C_5H_{11}ONO$ is the same (linestrengths $f_{1\text{-}C4H9ONO,376nm} = 0.0030$, $f_{2\text{-}C5H11ONO} = 0.0028$). A UV lamp and a Si photodiode were placed on opposite sides of a quartz cell (path length L_{UV}=0.2125 cm). The voltage of the detector was recorded in the absence and presence of RONO. From these measurements, $[RONO]_{gasline}$, the concentration of alkyl nitrite in the bubbler gas line, can be calculated using Equation 8.12:

$$[\text{RONO}]_{gasline} = \frac{1}{\sigma_{RONO,254nm} L_{UV}} \ln\left(\frac{I_0}{I}\right), \tag{8.12}$$

where I_0 is the detector voltage in the absence of RONO, and I is the detector voltage in the presence of RONO.

The second method to obtain [RONO] makes use of the thermodynamic properties of the alkyl nitrites. The first step is to calculate the vapor pressure of RONO in the bubbler. Assuming that the enthalpy of vaporization is independent of temperature, the vapor pressure can be calculated by Equation 8.13:

$$p_{vap} = p_{ref} \exp\left[\frac{-\Delta H_{vap,ref}}{R}\left(\frac{1}{T_{bubbler}} - \frac{1}{T_{ref}}\right)\right], \tag{8.13}$$

where p_{vap} is the vapor pressure of RONO in the bubbler, p_{ref} is the vapor pressure at a reference temperature, $\Delta H_{vap,ref}$ is the enthalpy of vaporization at a reference temperature, R is the universal gas constant, $T_{bubbler}$ is the temperature of the bubbler, and T_{ref} is the reference temperature. For our experiments, *n*-butyl nitrite has a vapor pressure of 760 torr at 351 K, with ΔH_{vap} = 37 kJ mol^{-1} (from the CRC handbook). Using these values with our bubbler temperature of 273 K gives us p_{vap} = 20.3 torr. Based on our results from Chapter 7, 2-pentyl nitrite has a vapor pressure of 760 torr at 350 K, with ΔH_{vap} = 41 kJ mol^{-1}. Using these values with our bubbler temperature gives us p_{vap} = 13.5 torr.

[RONO] can then be calculated by Equation 8.14:

$$[\mathrm{RONO}]_{gasline} = p_{vap}\left(3.24\times10^{16}\,\frac{\mathrm{molec}/\mathrm{cm}^3}{\mathrm{Torr}}\right). \tag{8.14}$$

With either method, [RONO] in the CRDS cell can be calculated by Equation 8.15:

$$[\mathrm{RONO}]_{CRDS} = [\mathrm{RONO}]_{gasline}\left(\frac{T_{bubbler}}{T_{cell}}\right)\left(\frac{f_{bubbler}}{\sum f_i}\right), \tag{8.15}$$

where $[\mathrm{RONO}]_{CRDS}$ is the concentration of the alkyl nitrite in the gas kinetics cell, $T_{bubbler}$ is the temperature of the bubbler (273 K), T_{cell} is the temperature of the gas kinetics cell (298 K), $f_{bubbler}$ is the gas flow through the bubbler, and $\sum f_i$ is the sum of all gas flows through the gas kinetics cell. Although the absolute [RONO] from Equations 8.12 and 8.14 are not equal, it can be shown that they are nearly proportional, and thus both methods should give approximately the same quality fits (and the same k_{isom}/k_{O2}).

Additionally, since we know the absolute [RONO], we can also calculate [RO•] using the results of Equations 8.1 and 8.15:

$$[\mathrm{RO}\bullet] = [\mathrm{RONO}]\left(\%_{photolysis}\right). \tag{8.16}$$

The third method to calculate [RONO] does not obtain an absolute value for [RONO], but rather a relative value for each data set, by measuring the background (excimer off) ringdown lifetime of a single frequency (3678 cm^{-1} for C_4H_9ONO, 3662 cm^{-1} for $C_5H_{11}ONO$). Assuming a pure sample of RONO (FTIR analysis of C_4H_9ONO shows that after freeze pumping, very low concentrations of other organic contaminants are present in the sample), the background gases only consist of N_2, O_2, and RONO. Thus, the absorbance can be fully attributed to RONO, and should be proportional to [RONO]. We can therefore obtain a relative [RONO] by Equation 8.17:

$$[\mathrm{RONO}]_{CRDS} \alpha \left(\frac{1}{\tau} - \frac{1}{\tau_0}\right)_{\bar{\nu}}, \tag{8.17}$$

where $1/\tau$ is the inverse ringdown lifetime measured with RONO present in the cell, and $1/\tau_0$ is the inverse ringdown lifetime in the absence of RONO. Both measurements must be made at the same frequency, $\bar{\nu}$. There may be drifts in the proportionality of Equation 8.17 over the course of an experiment; therefore, an entire day's worth of data cannot be scaled to the first set of data taken. Rather, each set of seven or eight points can be scaled to each other. Such a method of scaling each set of data separately from each other is valid because at the end of our analysis, we only care about relative absorbances, not the absolute absorbances and concentrations.

Note that since we are only obtaining a relative [RONO] by scaling to the absorption background, we cannot obtain the absolute value of [RO•].

Rescaling of Alkoxy Concentrations and Calculation of Relative Absorbance A_0/A

We are interested in how the [HOROO•] changes with $[O_2]$. Rather than rely on an absolute measurement of [HOROO•], we can measure the fraction $[HOROO•]_0/[HOROO•]$; that is, the concentration of HOROO• at "$[O_2] = 0$" compared to [HOROO•] at the $[O_2]$ of interest. This is equivalent to comparing the ν_1 absorbance for each condition, A_0/A.

A_0/A is determined by three steps: measurement of the peak absorbance of HOROO• (in actuality, any primary or secondary isomerization product with an OH group), scaling of the absorbance to [RONO], and conversion of the scaled absorbances to A_0/A.

Absorbances were determined by measuring $\left(\frac{1}{\tau_{exon}} - \frac{1}{\tau_{exoff}}\right)_{\bar{\nu}}$, the difference in inverse ringdown lifetimes between the CRDS cell contents after photolysis (excimer on, or "exon") and before photolysis (excimer off, or "exoff"), at the peak absorption by HOROO•, $\bar{\nu}$. We use these values directly as a measure of the isomerization product formed.

It is theoretically possible to convert these values to [HOROO•] by Equation 8.18:

$$[\text{HOROO•}] = \frac{1}{\sigma_{\bar{\nu}} c} \frac{L_{opt}}{L_{phot}} \left(\frac{1}{\tau_{exon}} - \frac{1}{\tau_{exoff}}\right)_{\bar{\nu}}, \qquad (8.18)$$

where $\sigma_{\bar{\nu}}$ is the absorption cross section of HOROO• at frequency $\bar{\nu}$, L_{opt} is the optical path length of the CRDS cell (distance between the mirrors), and L_{phot} is the width of the photolysis beam (and therefore the path length of HOROO•). However, the quantum chemistry calculations presented in Chapter 9 show that the absorption cross sections of

HOROO• and the end-product HORCHO are quite different than •ROH (hydroxy alkyl radicals), ROH (alcohols), or other molecules with an –OH group. There is no guarantee that the OH stretch peak of HOROO• matches any other OH stretch peak in the literature. It is therefore inappropriate to assign a cross section to the peak of HOROO•, even with theoretical integrated absorption cross sections available.

In order to obtain quantitatively correct relative absorbances, we must account for the fact that each piece of data has a different [RONO] based on the gas flows, UV measurements, and background absorptions (Equations 8.12, 8.14, 8.17). We therefore scale each of the measured absorbances to a reference [RONO] using Equation 8.19:

$$\left(\frac{1}{\tau}-\frac{1}{\tau_0}\right)_{scaled}=\frac{[\mathrm{RONO}]_{reference}}{[\mathrm{RONO}]_{measured}}\left(\frac{1}{\tau}-\frac{1}{\tau_0}\right)_{measured}, \tag{8.19}$$

where $\left(\frac{1}{\tau}-\frac{1}{\tau_0}\right)_{scaled}$ is the scaled difference in ringdown times, $[\mathrm{RONO}]_{\mathrm{reference}}$ is the reference concentration of RONO (taken to be the first [RONO] in each data set) from Equations 8.12, 8.14, 8.17, and $[\mathrm{RONO}]_{\mathrm{measured}}$ is the concentration of RONO for the current piece of data, using the same equation for determining [RONO] as the reference equation.

Once the scaled absorbances have been calculated, A_0/A can be calculated. A plot of $\left[\left(\frac{1}{\tau}-\frac{1}{\tau_0}\right)_{scaled}\right]^{-1}$ vs $[O_2]$ was made for each data set of 7–10 data points, using each scaling method. The simplest analysis of alkoxy relative rate experiments predicts that A_0/A should depend linearly on $[O_2]$. (As will be shown later, nonlinearity is observed only in the case of significant prompt isomerization). Linear regression was performed

for each plot, and the y-intercept of each plot, $\left[\left(\frac{1}{\tau}-\frac{1}{\tau_0}\right)_{scaled}\right]^{-1}_{[O_2]=0}$, was taken to be $A_0/A = 1$, the maximum [HOROO•] absorbance possible for a given [RO•]. Thus, A_0/A can be calculated by Equation 8.20:

$$\frac{A_0}{A} = \frac{\left(\frac{1}{\tau_{exon}}-\frac{1}{\tau_{exoff}}\right)_{scaled}}{\left(\frac{1}{\tau_{exon}}-\frac{1}{\tau_{exoff}}\right)_{[O_2]=0}}. \qquad (8.20)$$

We cannot use all of our A_0/A vs $[O_2]$ data in our linear regressions. Non-linearities are observed for $[O_2] < 10^{17}$ molec cm^{-3} due to the difference in absorption cross sections of HOR• and HOROO• (spectra shown in Chapter 7, explanation of nonlinearities in Chapter 9). As will be shown in the derivation of A_0/A vs $[O_2]$ section, prompt isomerization will cause non-linearity at high $[O_2]$. **Taking both factors into account, we only use data points in the range 1.0×10^{17} molec cm^{-3} < $[O_2]$ < 1.7×10^{19} molec cm^{-3} in our linear regressions.**

Choosing the Best Fits to Obtain the Overall Data Set for k_{isom}/k_{O2}

As stated in the previous section, it is important to scale the points within each experimental data set to [RONO] to ensure that the A_0/A values are quantitatively correct. Three equally valid scaling methods were presented, and in the absence of an overall "best" method, we must determine a way to determine which scaling method to use.

Performing linear regression on each data set of 7–10 points gives individual values and uncertainties of k_{isom}/k_{O2} for each fit. One of the three scaling methods yields the lowest uncertainty; this scaling method was chosen as the "best" scaling method. The

data points A_0/A vs $[O_2]$ for each of the "best" points were then compiled into one large data set for both *n*-butoxy and 2-pentoxy. Five plots (and thus five k_{isom}/k_{O2} values) were then computed using five overall data sets: unscaled data, scaling to UV measurements, scaling to thermodynamics, scaling to RONO background, and using the data from the best fits.

Derivation of Dependence of A_0/A on $[O_2]$

The absorbances that we are observing in the CRDS alkoxy experiments are measures of the ν_1 band (OH stretch) of the alkoxy isomerization product HOROO•, formed from "normal" isomerization (Reaction 8.4) and prompt isomerization (Reaction 8.8). Our goal in this section is to determine how the measured absorbance depends on $[O_2]$ given the six possible reactions of alkoxy (Reactions 8.4–8.9). We first show that prompt decomposition reduces the amount of starting alkoxy (and therefore the absolute absorbance measured), but does not affect A_0/A or any of the relative rate measurements. We then analyze the remaining five pathways.

Neglect of Prompt Decomposition

We begin our experiments by photolyzing an alkyl nitrite RONO into our alkoxy radical RO•. The alkoxy radicals that are initially formed [RO•] can be calculated from Equation 8.21:

$$[\mathrm{RO}\bullet]_0 = [\mathrm{RONO}] \times \%_{photolysis}, \tag{8.21}$$

where $\%_{photolysis}$ can be calculated from Equation 8.1.

A fraction newly formed alkoxy radicals will promptly decompose (Reaction 8.9). Define this fraction as ϕ_{pd}. Then the amount of alkoxy radicals left for reaction, $[RO\bullet]_{available}$, is given by Equation 8.22:

$$\left[RO\bullet\right]_{available} = \left[RO\bullet\right]_0 \times \left(1-\phi_{pd}\right) = \left[RONO\right] \times \left[\%_{photolysis} \times \left(1-\phi_{pd}\right)\right]. \quad (8.22)$$

For a constant photolysis wavelength, $\%_{photolysis}$ and ϕ_{pd} are constant. We can therefore define an effective photolysis ratio, $\%_{photolysis,eff}$, calculated from Equation 8.23:

$$\%_{photolysis,eff} = \%_{photolysis,eff} \times \left(1-\phi_{pd}\right). \quad (8.23)$$

Substituting Equation 8.23 into Equation 8.22 gives us

$$\left[RO\bullet\right]_{available} = \left[RONO\right] \times \%_{photolysis,eff}. \quad (8.24)$$

The effects of prompt decomposition can be accounted for entirely in the photolysis ratio calculation. Therefore, prompt decomposition will have no effect on the relative kinetics analysis.

Prompt decomposition should not affect the OH stretch experiment at all, because the decomposition products cannot form secondary products with –OH groups on the timescales of Mollner's experiments (20–110 μs).[30] However, it may affect the A-X spectroscopy and kinetics experiments. One of the products of decomposition is an alkyl radical. In the presence of O_2, a rapid association reaction will occur, resulting in formation of an alkylperoxy radical (Reaction 8.25).

$$R\bullet + O_2 \longrightarrow RO_2\bullet \quad (8.25)$$

These peroxy radicals will have their own A-X spectroscopic bands, and may interfere with the HOROO• spectrum. It is therefore important to note that while prompt

decomposition will not fundamentally affect the relative kinetics experiments, spectroscopic interference still needs to be considered.

Treatment of the remaining pathways

Next consider the remaining 5 alkoxy reactions: isomerization, reaction with O_2, decomposition, recombination with NO, and prompt isomerization (Reactions 8.4–8.8). Here, we show that the relative rate constants k_{isom}/k_{O2} can be determined from the relative absorbances A_0/A.

We have defined A as the OH stretch absorbance for a given $[O_2]$, and A_0 as the OH stretch absorbance for "$[O_2] = 0$" (actually an extrapolated value due to the low $[O_2]$ anomaly described in Chapter 9). By Beer's Law, the ratio A_0/A is

$$\frac{A_0}{A} = \frac{\sigma_{HOROO\bullet} L_{phot} \left([\text{HOROO}\bullet] \right)_{[O_2]=0}}{\sigma_{HOROO\bullet} L_{phot} [\text{HOROO}\bullet]} = \frac{\left([\text{HOROO}\bullet] \right)_{[O_2]=0}}{[\text{HOROO}\bullet]}, \tag{8.26}$$

where $\sigma_{HOROO\bullet}$ is the ν_1 cross section of HOROO• and L_{phot} is the photolysis length (sample length of HOROO•). Furthermore, we can convert [HOROO•] to an isomerization yield ϕ_{isom} by Equation 8.27:

$$\frac{A_0}{A} = \frac{\left([\text{HOROO}\bullet] \right)_{[O_2]=0} \Big/ [\text{RO}]_0}{[\text{HOROO}\bullet] \Big/ [\text{RO}]_0} = \frac{\left(\phi_{isom} \right)_{[O_2]=0}}{\phi_{isom}}. \tag{8.27}$$

In Equation 8.27, ϕ_{isom} is defined as the isomerization yield of alkoxy radicals that did not undergo prompt decomposition. Using the five remaining alkoxy reactions

(Reactions 8.4–8.8), we obtain

$$\phi_{isom} = \phi_{pi} + \left(1 - \phi_{pi}\right) \frac{k_{isom}}{k_{isom} + k_{O_2}\left[\mathrm{O_2}\right] + k_{decomp} + k_{NO}\left[\mathrm{NO}\right]}, \tag{8.28}$$

where ϕ_{pi} is the fraction of alkoxy radicals that promptly isomerize (Reaction 8.8), and k_{isom}, k_{O2}, k_{decomp}, and k_{NO} represent the rate constants for alkoxy isomerization, reaction with O_2, decomposition, and reaction with NO respectively.

Substituting Equation 8.28 into Equation 8.27 gives us

$$\frac{A_0}{A} = \frac{\left(\dfrac{\dfrac{k_{O_2}}{k_{isom}}}{1 + \dfrac{k_{NO}\left[\mathrm{NO}\right]}{k_{isom}} + \dfrac{k_{decomp}}{k_{isom}}} \right)\left[\mathrm{O_2}\right] + 1}{\left(\dfrac{\phi_{pi}\dfrac{k_{O_2}}{k_{isom}}}{1 + \phi_{pi}\left(\dfrac{k_{NO}\left[\mathrm{NO}\right]}{k_{isom}} + \dfrac{k_{decomp}}{k_{isom}} \right)} \right)\left[\mathrm{O_2}\right] + 1}. \tag{8.29}$$

Although the relationship between A_0/A and $[O_2]$ is nonlinear, Equation 8.29 shows that we can extract k_{isom}/k_{O2} from our CRDS absorbance data.

The typical analysis of alkoxy chemistry[148, 154-156, 159, 160] assumes that decomposition, reaction with NO, and prompt isomerization are all negligible. In this limit, we recover the "classic" equation used in alkoxy relative kinetics analysis:

$$\lim_{k_{decomp}, k_{NO}, \phi_{pi} \to 0} \left(\frac{A_0}{A} \right) = \frac{k_{O_2}}{k_{isom}}\left[\mathrm{O_2}\right] + 1. \tag{8.30}$$

Determination of k_{isom}/k_{O2}

When only isomerization and reaction with O_2 are considered, a plot of A_0/A vs $[O_2]$ is linear with slope k_{O2}/k_{isom} (Equation 8.30). We can therefore calculate k_{isom}/k_{O2} by Equation 8.31:

$$\frac{k_{isom}}{k_{O_2}} = \left[\frac{\partial\left(\frac{A_0}{A}\right)}{\partial[\mathrm{O_2}]} \right]^{-1} . \tag{8.31}$$

The full dependence of A_0/A on $[O_2]$ (Equation 8.29) is approximately linear at low $[O_2]$, and the slope of the line should be related to k_{isom}/k_{O2}. First start by calculating the derivative of Equation 8.29:

$$\left(\frac{\partial\left(\frac{A_0}{A}\right)}{\partial[\mathrm{O_2}]} \right) = \frac{\frac{k_{O_2}}{k_{isom}}}{1+\frac{k_{decomp}}{k_{isom}}+\frac{k_{NO}[\mathrm{NO}]}{k_{isom}}} \times \frac{\left(1-\phi_{pi}\right)\left[1+\phi_{pi}\left(\frac{k_{decomp}}{k_{isom}}+\frac{k_{NO}[\mathrm{NO}]}{k_{isom}}\right)\right]}{\left[1+\phi_{pi}\left(\frac{k_{O_2}}{k_{isom}}[\mathrm{O_2}]+\frac{k_{decomp}}{k_{isom}}+\frac{k_{NO}[\mathrm{NO}]}{k_{isom}}\right)\right]^2} . \tag{8.32}$$

At low $[O_2]$, Equation 8.32 reduces to

$$\left(\frac{\partial\left(\frac{A_0}{A}\right)}{\partial[\mathrm{O_2}]} \right)_{[\mathrm{O_2}]=0} = \frac{\frac{k_{O_2}}{k_{isom}}}{\left[1+\frac{k_{decomp}}{k_{isom}}+\frac{k_{NO}[\mathrm{NO}]}{k_{isom}}\right]} \times \left[\frac{\left(1-\phi_{pi}\right)}{1+\phi_{pi}\left(\frac{k_{decomp}}{k_{isom}}+\frac{k_{NO}[\mathrm{NO}]}{k_{isom}}\right)} \right] . \tag{8.33}$$

Solving Equation 8.33 for k_{isom}/k_{O2} gives

$$\frac{k_{isom}}{k_{O_2}} = \left[\left(\frac{\partial\left(\frac{A_0}{A}\right)}{\partial[\mathrm{O_2}]} \right)_{[\mathrm{O_2}]=0} \right]^{-1} \times \left[\frac{1}{1+\frac{k_{decomp}}{k_{isom}}+\frac{k_{NO}[\mathrm{NO}]}{k_{isom}}} \right] \times \left[\frac{\left(1-\phi_{pi}\right)}{1+\phi_{pi}\left(\frac{k_{decomp}}{k_{isom}}+\frac{k_{NO}[\mathrm{NO}]}{k_{isom}}\right)} \right] . \tag{8.34}$$

According to Equation 8.34, the true k_{isom}/k_{O2} is the product of three terms. The first term in Equation 8.34 is the k_{isom}/k_{O2} that was calculated by assuming that the only

important alkoxy reactions are isomerization and reaction with O_2 (the typical analysis found in the literature). The second and third terms are "correction" factors for the other reaction pathways and prompt isomerization respectively. We can rewrite Equation 8.34:

$$\frac{k_{isom}}{k_{O_2}} = \left[\left(\frac{\partial \left(\frac{A_0}{A} \right)}{\partial [\mathrm{O_2}]} \right)_{[\mathrm{O_2}]=0} \right]^{-1} \times X_{kin} \times X_{prompt}, \tag{8.35}$$

where

$$X_{kin} = \frac{1}{1 + \frac{k_{decomp}}{k_{isom}} + \frac{k_{NO}[\mathrm{NO}]}{k_{isom}}}, \tag{8.36}$$

$$X_{prompt} = \frac{\left(1 - \phi_{pi}\right)}{1 + \phi_{pi}\left(\frac{k_{decomp}}{k_{isom}} + \frac{k_{NO}[\mathrm{NO}]}{k_{isom}} \right)}, \tag{8.37}$$

X_{kin} is the correction factor for the missing kinetic reaction pathways (decomposition, reaction with NO), and X_{prompt} is the correction factor for prompt isomerization.

We can calculate the true $k_{\mathrm{isom}}/k_{\mathrm{O2}}$ by a relatively simple procedure. First, we perform linear regression to the relative kinetics data set to obtain the slope $\left(\frac{\partial \left(\frac{A_0}{A} \right)}{\partial [\mathrm{O_2}]} \right)_{[\mathrm{O_2}]=0}$. Then, we apply the correction factors X_{kin} and X_{prompt} to obtain $k_{\mathrm{isom}}/k_{\mathrm{O2}}$.

Results

The results from this reanalysis are presented in four parts. First, a selected set of gas flow conditions is shown in order to illustrate how [O_2], [RONO], and [RO•] change

between the initial analysis and the reanalysis performed in this document. Second, a selected plot of A_0/A vs $[O_2]$ for an individual data set is shown to illustrate the changes in the plots between the initial analysis and the reanalysis, and to compare scaling methods. Third, the plots of A_0/A vs $[O_2]$ for the overall data sets of *n*-butoxy and 2-pentoxy are shown. Fourth, the best value of k_{isom}/k_{O2} is derived by using our CRDS data and Equation 8.34, the full dependence of our relative kinetics data on $[O_2]$.

Selected Gas Flow Data

Combining the *n*-butoxy and 2-pentoxy experiments, 903 sets of gas flows and concentrations were recalculated; therefore, all of the recalculated data cannot be presented in this document. Instead, one set of experimental conditions will be reported in order to illustrate how $[O_2]$, [RONO], and [RO•] change between the initial analysis and this reanalysis.

Table 8.2 contains the reanalyzed gas flows and concentrations from a single experimental scan, while Table 8.3 contains a comparison of $[O_2]$, [RONO], and [RO•] between the initial analysis and the reanalysis.

Table 8.2. One set of gas flow conditions (from 9/28/06, Scan 1), p = 670 torr

Flow	Gas	Function	sccm/V	$V_{0,i}$	V_i	Flow (sccm)	[gas] (molec cm^{-3})
1	N_2	Dilution	2182.9	0.16	2.73	5610	1.56×10^{19}
2	N_2	L-purge	184.2	0.023	4.01	734	2.04×10^{18}
3	O_2	Dilution	-1940.6	-0.073	-0.36	557	1.55×10^{18}
4	N_2	bubbler	101.5	0.42	1.92	152	4.23×10^{17}
5	N_2	R-purge	415.8	0.165	1.99	759	2.11×10^{18}

Table 8.3. Comparison of the initial analysis of one set of gas concentrations to the reanalysis

	$[O_2]$ (molec cm^{-3})	[RONO] (molec cm^{-3})	[RO•] (molec cm^{-3})
Initial Values	1.68×10^{18}	6.8×10^{15}	0.68×10^{14}
Reanalyzed Values	1.56×10^{18}	1.1×10^{16} (UV) 1.2×10^{16} (thermo)	1.9×10^{14} 2.0×10^{14}

Examination of Table 8.3 reveals striking differences between the initially calculated experimental conditions and the recalculated conditions. As explained in the introduction, the recalculated $[O_2]$ is less than the initially calculated $[O_2]$ (in this example, by 7%) because the right purge flow was not initially used in the calculation of total gas concentrations. The recalculations of [RONO] based on the UV measurements and thermodynamic parameters are greater than the values recorded in the lab notebook (in this example, by a factor of 1.5). It is likely that this discrepancy comes from two errors: the miscalculation of gas flows and concentrations that also affect the $[O_2]$ calculation, and the use of incorrect flowmeter calibrations in the photolysis calculator and/or the gas flow calculator. This problem affects all of the N_2 bath gas data and much of the Ar bath gas data. Finally, the discrepancies in [RO•] are even greater than the previous two errors (in this case, a factor of 2.6), caused by the above two errors, and the miscalculation of photolysis flux described in the introduction.

Putting all of these errors together, we expect the derived value of k_{isom}/k_{O2} to change dramatically. The changes in $[O_2]$ directly affect the plot of A_0/A vs $[O_2]$, while the changes in [RONO] will affect how each individual data point is scaled. Because our data do not depend on the absolute value of [RO•] (we do not directly measure the kinetics of HOROO• formation and decay in the OH stretch experiment), the errors in [RO•] will not affect k_{isom}/k_{O2}.

Recalculations on each data point of the entire alkoxy data set gives similar results to the example shown above. The actual $[O_2]$ values are lower than the previously recorded values by a factor of 7%–10%, [RONO] is higher than the previously recorded values by a factor of 1.5–2, and [RO•] is higher than the previous values by a factor of 2–3.

How Scaling Method Affects A_0/A vs $[O_2]$

Since [RONO] may vary during the course of an experiment, each data point in a single data set must be scaled to a reference [RONO]. As stated in the introduction, there are three methods that can be used: scaling to the UV absorption measurements (Equation 8.4), scaling by thermodynamic parameters (Equation 8.6), and scaling by background nitrite absorption (Equation 8.9). Since all three methods are equally valid ways to scale data points, the strategy is to use each individual method to scale the data points and determine which scaling method gives the best fit.

Figure 8.2 shows four plots of A_0/A vs $[O_2]$ for the same data set, without any scaling, and using each of the three described scaling methods. This data set was chosen to show that scaling method can often have a large effect on the quality of linear fit. However, for a typical data set, the UV and thermodynamic scaling methods usually gave similar uncertainties and $\left[\frac{\partial\left(\frac{A_0}{A}\right)}{\partial[O_2]}\right]^{-1}$ (calculated as the ratio of the y-intercept to slope, or *int/slope*) values. Scaling to the CRDS background usually gave *int/slope* values with the largest uncertainties, possibly due to interference by other molecules in the IR region.

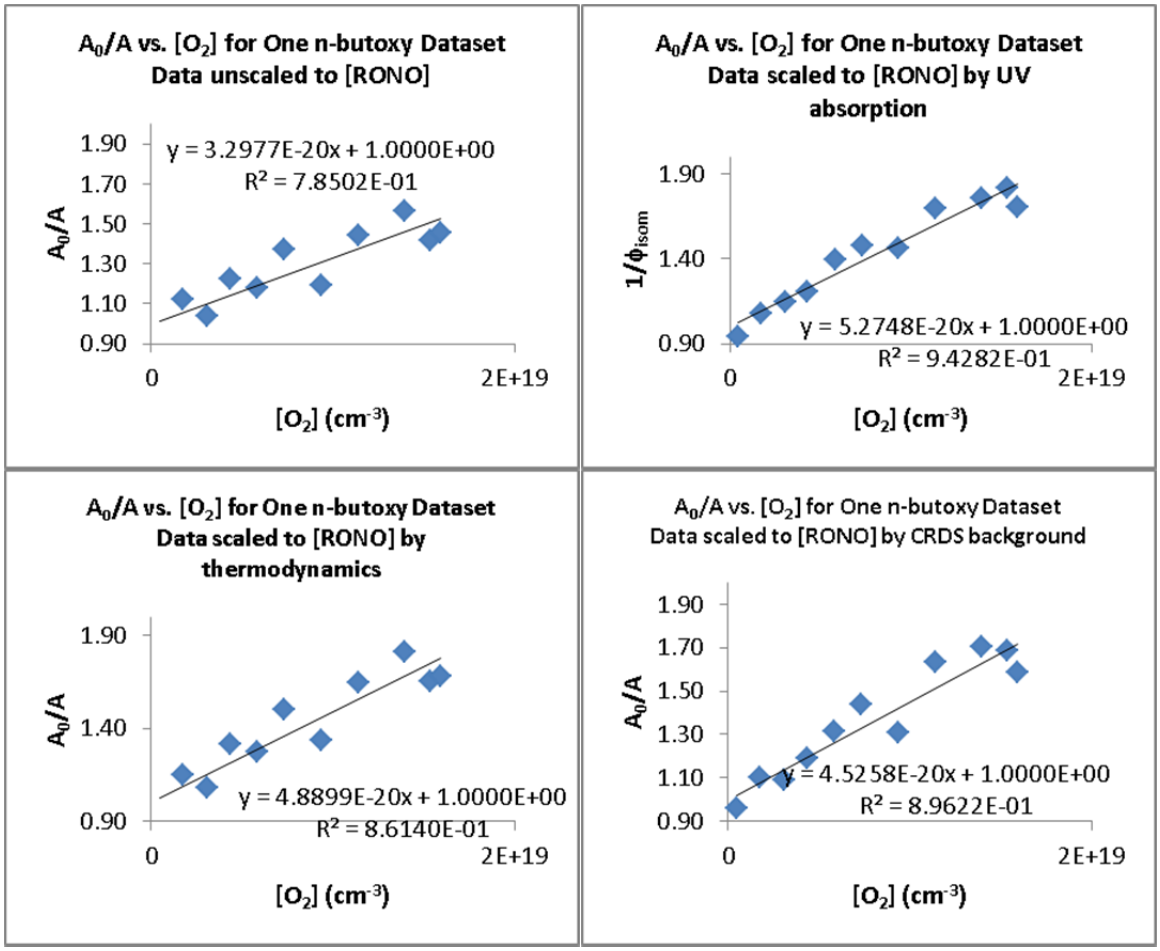

Figure 8.2. Plots of A_0/A vs $[O_2]$ for one n-butoxy data set (9/28/06, scans 73–105) using different scaling methods. Upper left: no scaling to [RONO], *int/slope* =$(3.0 \pm 0.6) \times 10^{19}$ cm^{-3} . Upper right: Scaling to [RONO] based on UV absorption measurements at 254 nm, *int/slope* = $(1.9 \pm 0.2) \times 10^{19}$ cm^{-3}. Lower left: Scaling to [RONO] based on thermodynamic parameters, *int/slope* = $(2.1 \pm 0.3) \times 10^{19}$ cm^{-3}. Lower right: Scaling to [RONO] based on CRDS background absorption at 3678 cm^{-1}, *int/slope* = $(2.2 \pm 0.3) \times 10^{19}$ cm^{-3}. All uncertainties are reported to 1σ. For this data set, scaling to UV absorption gives the smallest uncertainty on k_{isom}/k_{O2}, although this is not true for all other data sets.

Visual inspection of the four plots in Figure 8.2 reveals that scaling to the UV absorption gives the best linear fit. Examination of the standard errors on the derived *int/slope* values confirms this point. The *int/slope* values, absolute 1σ uncertainties, and 1σ percent uncertainties for each fit are $(3.0 \pm 0.6) \times 10^{19}$ cm^{-3} (18%) for the unscaled data, $(1.9 \pm 0.2) \times 10^{19}$ cm^{-3} (9%) for the UV scaled data, $(2.1 \pm 0.3) \times 10^{19}$ cm^{-3} (15%)

for the thermodynamics scaled data, and (2.2 ± 0.3) × 10^{19} cm^{-3} (12%) for the background scaled data. For this data set, scaling to the UV measurements yields the best linear fit. This is not the best method for every data set: some sets are best fit by scaling to the thermodynamic parameters, and a few sets are best fit to the background CRDS absorptions. None of the data sets are best fit by the unscaled data points.

Overall Data Set of A_0/A vs $[O_2]$ and Calculated int/slope

The full data sets of A_0/A vs $[O_2]$ consist of 191 data points for *n*-butoxy and 76 data points for 2-pentoxy. Only 177 data points for *n*-butoxy were used for the linear fits to determine k_{isom}/k_{O2}. Six points were measured at $[O_2] < 1.7 \times 10^{17}$ molec cm^{-3}, and are therefore subject to the low $[O_2]$ anomaly described in Chapter 9. Eight of the points were measured at $[O_2] > 1.7 \times 10^{19}$ molec cm^{-3}, and therefore may be subject to nonlinearities in A_0/A vs $[O_2]$ due to prompt isomerization. In contrast, all of the data points for 2-pentoxy were used because the $[O_2]$ used fell within the linear regime for A_0/A vs $[O_2]$.

There are five methods that can be used to generate full data sets of A_0/A vs $[O_2]$, and therefore to determine *int/slope*, based on the scaling procedures in the previous section. Four of the methods are to simply use the A_0/A values derived from the previous section (unscaled, scaled to UV absorption, scaled to thermodynamics, scaled to background CRDS absorption) to create four data sets of A_0/A vs $[O_2]$. The fifth method is to use the A_0/A values from each individual data set that gave the best linear fit, and combine each of these individual sets of A_0/A values into an overall data set. Each data set can then be fit to Equation 8.13 to obtain A_0/A. Presumably, the fifth data set should give a value of *int/slope* with the lowest uncertainty.

The five plots of A_0/A vs $[O_2]$ for *n*-butoxy using each scaling method are shown in Figure 8.3, while the five plots for 2-pentoxy are shown in Figure 8.4. As expected, using the best fits from each individual data set give an overall data set with the lowest uncertainty on *int/slope*. Additionally, scaling to UV absorption measurements or thermodynamic parameters yields the same absolute value of *int/slope*, but with slightly higher uncertainties. The agreement between *int/slope* values strongly implies that using the best fits from each individual data set is a valid method for generating an overall data set.

Tables 8.4 and 8.5 summarize the derived *int/slope* parameters using each scaling method. By using the A_0/A generated from the best scaling method for each individual data set, **we obtain *int/slope* = (1.81 ± 0.15) × 10^{19} cm^{-3} for *n*-butoxy, and (3.86 ± 0.45) × 10^{19} cm^{-3} for 2-pentoxy (reported to 2σ error).**

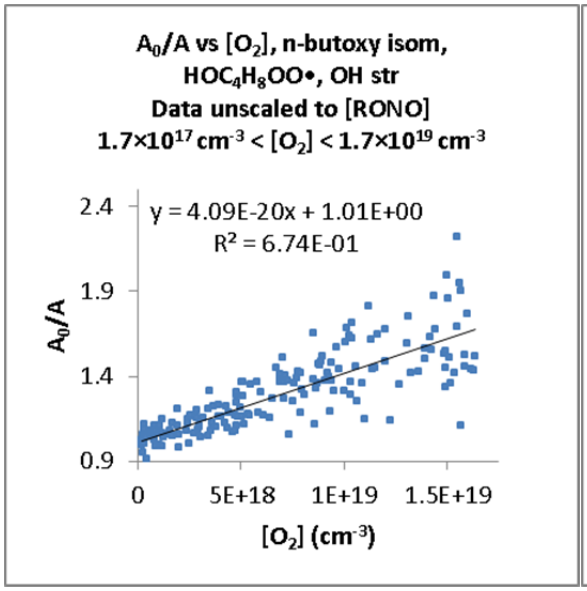
A0/A vs [O2], n-butoxy isom,
HOC4H8OO•, OH str
Data unscaled to [RONO]
1.7×10^17 cm^-3 < [O2] < 1.7×10^19 cm^-3
y = 4.09E-20x + 1.01E+00
R² = 6.74E-01
A0/A
2.4
1.9
1.4
0.9
0
5E+18
1E+19
1.5E+19
[O2] (cm^-3)

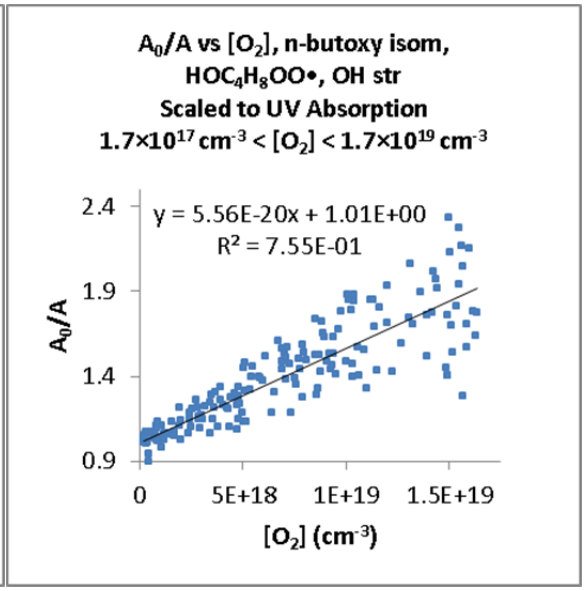
A0/A vs [O2], n-butoxy isom,
HOC4H8OO•, OH str
Scaled to UV Absorption
1.7×10^17 cm^-3 < [O2] < 1.7×10^19 cm^-3
y = 5.56E-20x + 1.01E+00
R² = 7.55E-01
A0/A
2.4
1.9
1.4
0.9
0
5E+18
1E+19
1.5E+19
[O2] (cm^-3)

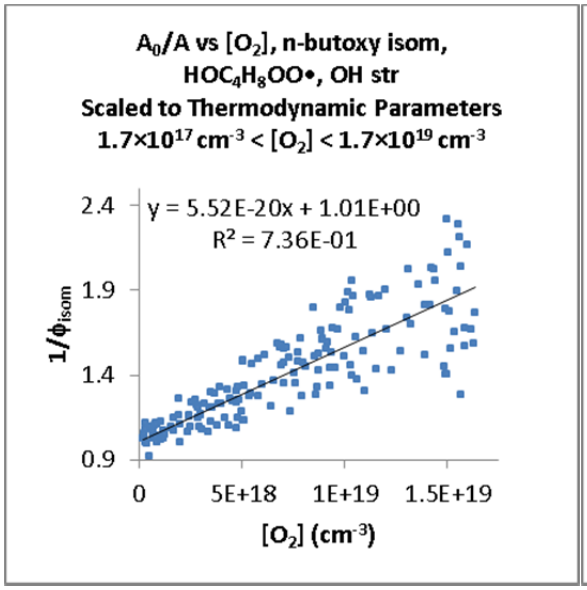
A0/A vs [O2], n-butoxy isom,
HOC4H8OO•, OH str
Scaled to Thermodynamic Parameters
1.7×10^17 cm^-3 < [O2] < 1.7×10^19 cm^-3
y = 5.52E-20x + 1.01E+00
R² = 7.36E-01
1/ϕisom
2.4
1.9
1.4
0.9
0
5E+18
1E+19
1.5E+19
[O2] (cm^-3)

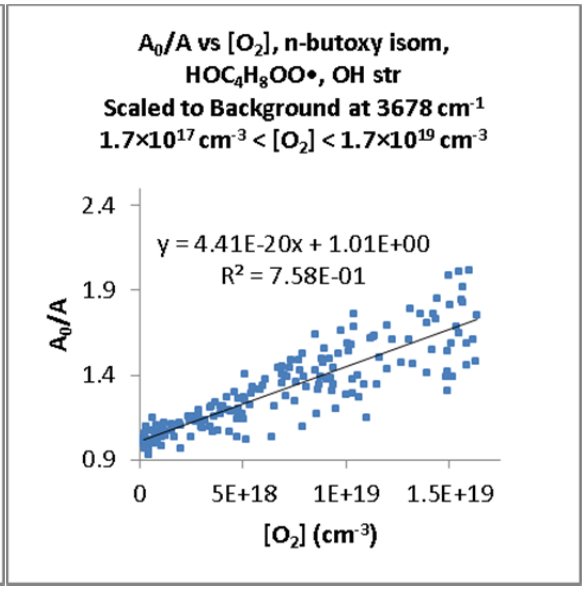
A0/A vs [O2], n-butoxy isom,
HOC4H8OO•, OH str
Scaled to Background at 3678 cm^-1
1.7×10^17 cm^-3 < [O2] < 1.7×10^19 cm^-3
y = 4.41E-20x + 1.01E+00
R² = 7.58E-01
A0/A
2.4
1.9
1.4
0.9
0
5E+18
1E+19
1.5E+19
[O2] (cm^-3)

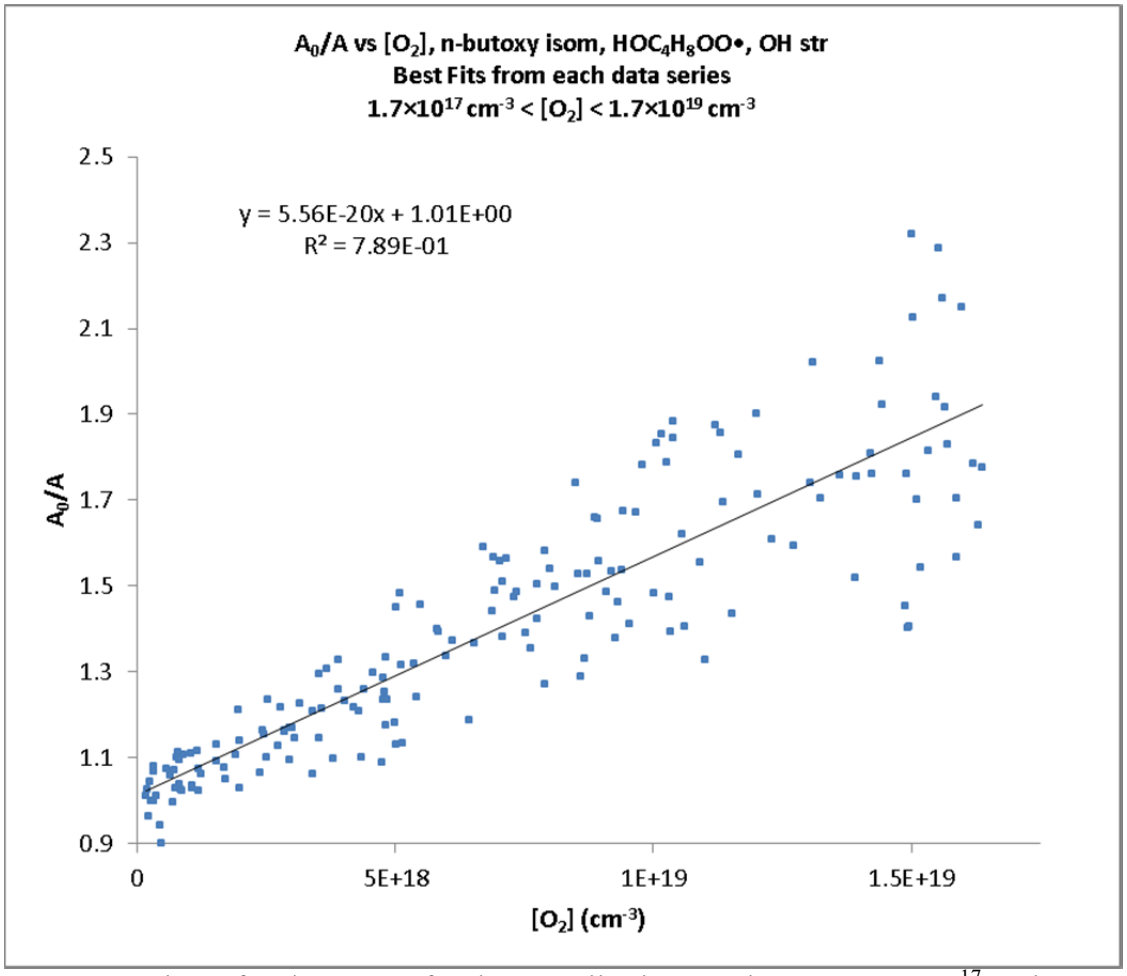

Figure 8.3. Plots of A_0/A vs $[O_2]$ for the overall *n*-butoxy data set, 1.7×10^{17} molec cm^{-3} < $[O_2]$ < 1.7×10^{19} molec cm^{-3}. On the previous page, Upper left: data unscaled to [RONO], *int/slope* = $(2.47 \pm 0.27) \times 10^{19}$ cm^{-3}. Upper right: data scaled by UV absorption measurements, *int/slope* = $(1.82 \pm 0.17) \times 10^{19}$ cm^{-3}. Bottom left: data scaled by thermodynamic parameters, *int/slope* = $(1.83 \pm 0.18) \times 10^{19}$ cm^{-3}. Bottom right: data scaled by CRDS background at 3678 cm^{-1}, *int/slope* = $(2.29 \pm 0.21) \times 10^{19}$ cm^{-3}. This page: Combination of best fits to each individual data set, *int/slope* = $(1.81 \pm 0.15) \times 10^{19}$ cm^{-3}. All errors reported as 2σ. Standard errors on the slopes and intercepts can be found in Table 8.4. Final figure adapted with permission from Sprague et al.[31] Copyright 2012 American Chemical Society.

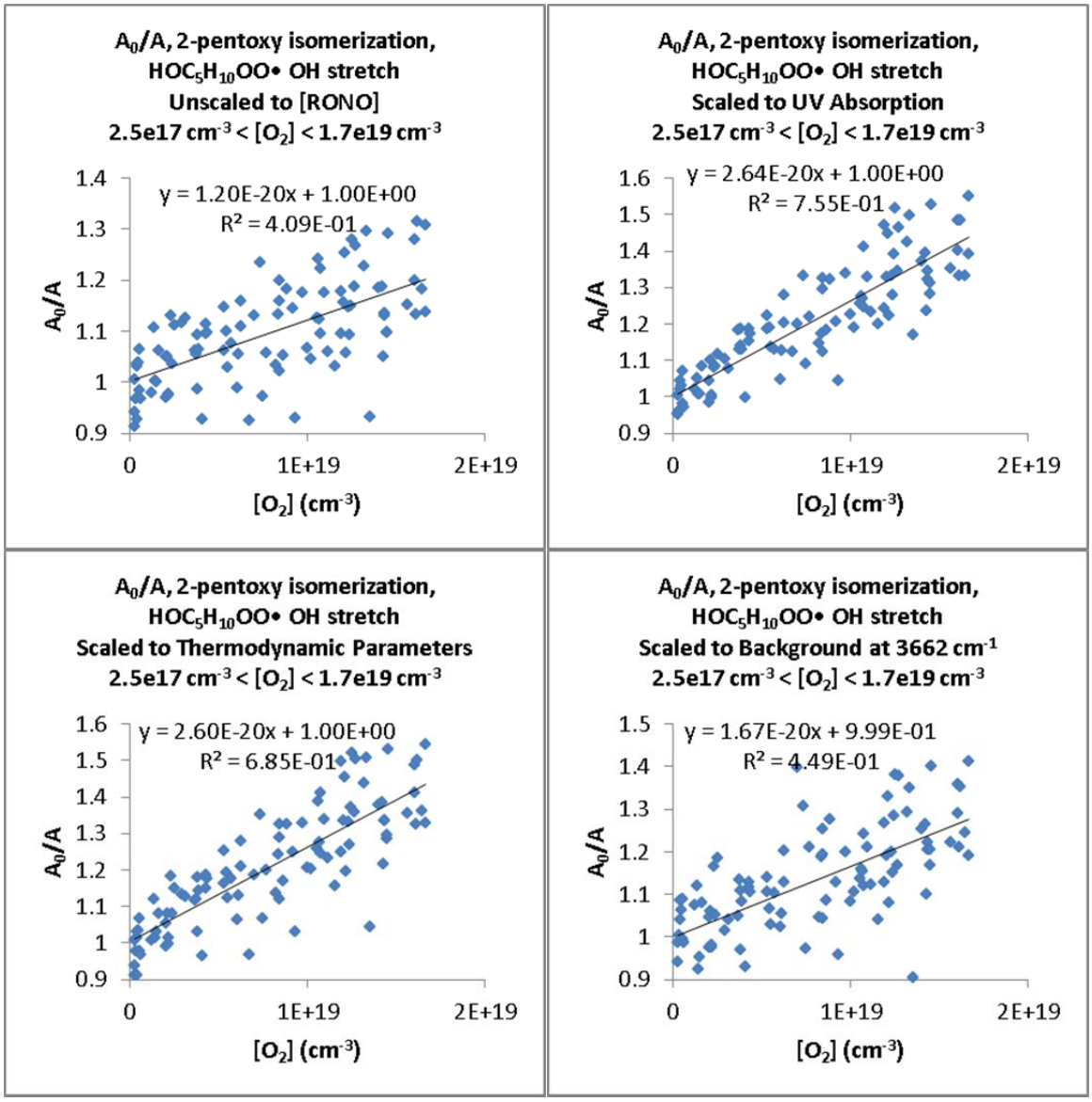
A0/A, 2-pentoxy isomerization,
HOC5H10OO• OH stretch
Unscaled to [RONO]
2.5e17 cm-3 < [O2] < 1.7e19 cm-3
y = 1.20E-20x + 1.00E+00
R² = 4.09E-01
A0/A
[O2] (cm-3)
A0/A, 2-pentoxy isomerization,
HOC5H10OO• OH stretch
Scaled to UV Absorption
2.5e17 cm-3 < [O2] < 1.7e19 cm-3
y = 2.64E-20x + 1.00E+00
R² = 7.55E-01
A0/A
[O2] (cm-3)
A0/A, 2-pentoxy isomerization,
HOC5H10OO• OH stretch
Scaled to Thermodynamic Parameters
2.5e17 cm-3 < [O2] < 1.7e19 cm-3
y = 2.60E-20x + 1.00E+00
R² = 6.85E-01
A0/A
[O2] (cm-3)
A0/A, 2-pentoxy isomerization,
HOC5H10OO• OH stretch
Scaled to Background at 3662 cm-1
2.5e17 cm-3 < [O2] < 1.7e19 cm-3
y = 1.67E-20x + 9.99E-01
R² = 4.49E-01
A0/A
[O2] (cm-3)

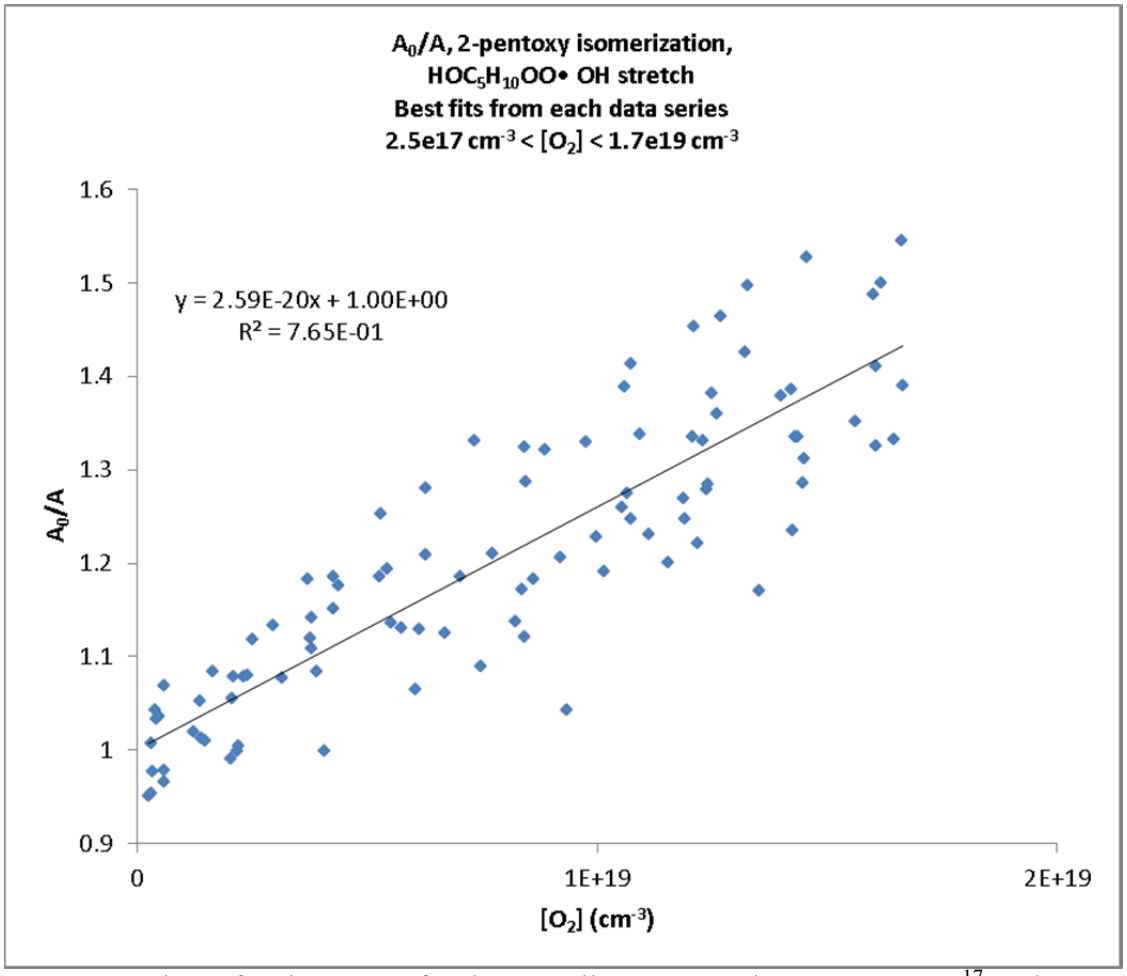

Figure 8.4. Plots of A_0/A vs $[O_2]$ for the overall 2-pentoxy data set, 1.7×10^{17} molec cm^{-3} < $[O_2]$ < 1.7×10^{19} molec cm^{-3}. On the previous page, Upper left: data unscaled to [RONO], *int/slope* = $(8.35 \pm 2.05) \times 10^{19}$ cm^{-3}. Upper right: data scaled by UV absorption measurements, *int/slope* = $(3.79 \pm 0.45) \times 10^{19}$ cm^{-3}. Bottom left: data scaled by thermodynamic parameters, *int/slope* = $(3.86 \pm 0.55) \times 10^{19}$ cm^{-3}. Bottom right: data scaled by CRDS background at 3678 cm^{-1}, *int/slope* = $(5.99 \pm 1.37) \times 10^{19}$ cm^{-3}. This page: combination of best fits to each individual data set, *int/slope* =$(3.86 \pm 0.45) \times 10^{19}$ cm^{-3}. All errors reported as 2σ. Standard errors on the slopes and intercepts can be found in Table 8.5. Final figure adapted with permission from Sprague et al.[31] Copyright 2012 American Chemical Society.

Table 8.4. Slopes, Intercepts, k_{isom}/k_{O2}, and Standard Errors for *n*-butoxy Data Fits

Scaling Method	Slope (10^{-20} cm^3)	St. Error (2σ) (10^{-20} cm^3)	y-Intercept	St. Error (2σ)	*int/slope* (10^{19} cm^{-3})	St. Error (2σ) (10^{19} cm^{-3})
Unscaled	4.09	0.42	1.00	0.04	2.47	0.27
UV	5.56	0.48	1.01	0.04	1.82	0.17
Thermo	5.52	0.50	1.01	0.04	1.83	0.18
Background	4.41	0.37	1.01	0.03	2.29	0.21
Best Fits	5.56	0.43	1.01	0.04	1.81	0.15

Table 8.5. Slopes, Intercepts, k_{isom}/k_{O2}, and Standard Errors for 2-pentoxy Data Fits

Scaling Method	Slope (10^{-20} cm^3)	St. Error (2σ) (10^{-20} cm^3)	y-Intercept	St. Error (2σ)	*int/slope* (10^{19} cm^{-3})	St. Error (2σ) (10^{19} cm^{-3})
Unscaled	1.20	0.29	1.00	0.03	8.35	2.05
UV	2.64	0.30	1.00	0.03	3.79	0.45
Thermo	2.60	0.36	1.00	0.03	3.86	0.55
Background	1.67	0.38	1.00	0.04	5.99	1.37
Best Fits	2.59	0.29	1.00	0.03	3.86	0.45

Required Parameters and Rate Constants

As shown in the *Methods* section, our relative kinetics data are expected to fit to Equation 8.29. We can extract k_{isom}/k_{O2} from this function by using Equations 8.35–8.37.

$$\frac{A_0}{A} = \frac{\left(\dfrac{\dfrac{k_{O_2}}{k_{isom}}}{1 + \dfrac{k_{NO}[\mathrm{NO}\bullet]}{k_{isom}} + \dfrac{k_{decomp}}{k_{isom}}} \right)[\mathrm{O_2}] + 1}{\left(\dfrac{\phi_{pi} \dfrac{k_{O_2}}{k_{isom}}}{1 + \phi_{pi}\left(\dfrac{k_{NO}[\mathrm{NO}\bullet]}{k_{isom}} + \dfrac{k_{decomp}}{k_{isom}} \right)} \right)[\mathrm{O_2}] + 1} \tag{8.29}$$

$$\frac{k_{isom}}{k_{O_2}} = \left[\left(\frac{\partial\left(\dfrac{A_0}{A}\right)}{\partial[\mathrm{O_2}]} \right)_{[\mathrm{O_2}]=0} \right]^{-1} \times X_{kin} \times X_{prompt} \tag{8.35}$$

$$X_{kin} = \frac{1}{1 + \frac{k_{decomp}}{k_{isom}} + \frac{k_{NO}[\mathrm{NO}\bullet]}{k_{isom}}} \tag{8.36}$$

$$X_{prompt} = \frac{\left(1 - \phi_{pi}\right)}{1 + \phi_{pi}\left(\frac{k_{decomp}}{k_{isom}} + \frac{k_{NO}[\mathrm{NO}]}{k_{isom}}\right)} \tag{8.37}$$

The parameters k_{decomp}, k_{isom}, k_{NO}, and ϕ_{pi} are summarized in Table 8.6. The justification for each rate constant is below the table. The justification for ϕ_{pi} is in the next section.

Table 8.6. – Rate constants, prompt process parameters, and 2σ uncertainties for *n*-butoxy and 2-pentoxy

		n-butoxy		2-pentoxy	
	Units	Best Value	Uncertainty (2σ)	Best Value	Uncertainty (2σ)
$\left[\left(\frac{\partial\left(\frac{A_0}{A}\right)}{\partial[\mathrm{O_2}]}\right)_{[\mathrm{O_2}]=0}\right]^{-1}$	10^{19} $\mathrm{cm^{-3}}$	1.81	0.15	3.86	0.45
k_{O2} [28, 142, 193]	10^{-14} $\mathrm{cm^3\ s^{-1}}$	1.40	0.70	0.80	0.40
k_{isom} (derived)	$10^5\ \mathrm{s^{-1}}$	2.53	1.28	3.09	1.59
k_{decomp} [117, 149]	$\mathrm{s^{-1}}$	600	300	2.0×10^4	1.0×10^4
$k_{\mathrm{NO}} \times [\mathrm{NO}]$ [32]	$\mathrm{s^{-1}}$	6640	3320	6640	3320
ϕ_{pi}		0.038	0.018	0.049	0.024

$\left[\left(\frac{\partial\left(\frac{A_0}{A}\right)}{\partial[\mathrm{O_2}]}\right)_{[\mathrm{O_2}]=0}\right]^{-1}$: Obtained from the fits presented in Figures 8.3 and 8.4.

***k*O2:** The recommended value and uncertainty for *n*-butoxy are taken from Atkinson's 2007 review paper.[142] The recommended value of the rate constant for 2-pentoxy is based on Balla's 1985 study of isopropoxy.[193] Atkinson recommends that all secondary alkoxy

radicals should have similar O_2 reaction rates.[142] Balla reports a 4% uncertainty on his value. However, I choose to use 50% uncertainty (same as *n*-butoxy) because of the possible differences between 2-pentoxy and isopropoxy. It can be shown that the effect of this choice on the overall uncertainty is negligible, less than a 1% change in the overall reported error on the final value of k_{isom}/k_{O2}.

k_{decomp}: The value and uncertainty of k_{decomp} for *n*-butoxy is taken from Curran's 2006 review paper, estimated as the difference between Curran's recommendation and Orlando's previous study.[149] Curran does not actually report an uncertainty, so the uncertainty was estimated on the basis of the Arrhenius plot in their paper (Figure 8.32). For 2-pentoxy, the uncertainty was estimated as the scatter in the theoretical rate constants available in the NIST kinetics database.[117] We chose a value of k_{decomp} that fell in the middle of the available rate constants.

k_{NO} × [NO]: Heicklen's recommendation is to use 3.32×10^{-11} cm^3 $molec^{-1}$ s^{-1} for all alkoxies.[32] The reported experimental data within his review paper have a scatter of roughly $\pm 0.4 \times 10^{-11}$ cm^3 $molec^{-1}$ s^{-1}. [NO] is taken to be equal to our [RO•] (2.0×10^{14} molec cm^{-3}). With few available studies on alkoxy recombination with NO, we choose to use an overall factor of 50% uncertainty. Similar to the uncertainty choice on k_{O2}, this increased uncertainty makes only a small difference in the overall reported uncertainty on k_{isom}/k_{O2}.

Prompt Isomerization: Determination of ϕ_{pi}

We have already observed that prompt isomerization will cause nonlinearities in the plot of A_0/A vs $[O_2]$ at high $[O_2]$ (Equation 8.29).

$$\frac{A_0}{A} = \frac{\left(\frac{\frac{k_{O_2}}{k_{isom}}}{1 + \frac{k_{NO}[\mathrm{NO}]}{k_{isom}} + \frac{k_{decomp}}{k_{isom}}} \right)[\mathrm{O_2}] + 1}{\left(\frac{\phi_{pi} \frac{k_{O_2}}{k_{isom}}}{1 + \phi_{pi}\left(\frac{k_{NO}[\mathrm{NO}]}{k_{isom}} + \frac{k_{decomp}}{k_{isom}} \right)} \right)[\mathrm{O_2}] + 1} \tag{8.29}$$

We can determine the best value of ϕ_{pi} by performing a fit of the entire alkoxy data sets to both the simple linear function (Equation 8.31) and the full non-linear form (Equation 8.29). We then calculate the reduced chi-squared variable, χ_ν^2, for the linear and nonlinear fits, defined by Equation 8.38:

$$\chi_\nu^2 = \frac{\chi^2}{\nu} = \frac{1}{N-p-1} \sum \frac{\left[y_i - y(x_i) \right]^2}{\sigma_i^2}, \tag{8.38}$$

where $\nu = N\text{-}p\text{-}1$ is the number of degrees of freedom, N is the number of data points in the overall alkoxy data set, p is the number of parameters to fit to, y_i is the measured value of the i^{th} point, $y(x_i)$ is the expected value of the i^{th} point based on the function being fit to, and σ_i is variance associated with the i^{th} point. In our cases, N = 177 for *n*-butoxy and N = 95 for 2-pentoxy. The number of parameters for each fit is 2 for the linear fits (k_{isom}, k_{O2}) and 3 for the nonlinear fits (k_{isom}, k_{O2}, and ϕ_{pi}). We then assume that each data point has the same fractional uncertainty on A_0/A, expressed in Equation 8.39:

$$\sigma_i = a \times \left(\frac{A_0}{A} \right), \tag{8.39}$$

where a is a multiplicative constant ($a < 1$). It can be shown that while the value of a affects the values of χ^2, it does not affect the final result for ϕ_{pi}. The best value of ϕ_{pi} is calculated by Equation 8.40:

$$\left[\chi_\nu^{\,2}\right]_{non-linear} = \left[\chi_\nu^{\,2}\right]_{linear} \times \left(1 + \frac{1}{\nu}\right). \tag{8.40}$$

The uncertainty is chosen to be the difference between the ϕ_{pi} determined from Equation 8.40 and the ϕ_{pi} which minimizes $\left[\chi_\nu^{\,2}\right]_{non-linear}$.

When we apply Equations 8.39 and 8.40 to the two alkoxy data sets, we obtain $\left[\chi_\nu^{\,2}\right]_{linear}$ = 0.830 for *n*-butoxy, and $\left[\chi_\nu^{\,2}\right]_{linear}$ = 0.365 for 2-pentoxy. The ϕ_{prompt} necessary to obtain the $\left[\chi_\nu^{\,2}\right]_{non-linear}$ described in Equation 8.40 are **ϕ_{pi} = 0.038 ± 0.018 for *n*-butoxy and ϕ_{pi} = 0.049 ± 0.024 for 2-pentoxy.**

Calculation of k_{isom}/k_{O2}, Comparison of Data Fits

With best values and uncertainties for each parameter in hand, we can calculate k_{isom}/k_{O2} and its uncertainty. The uncertainty is calculated by propagating the individual parameter uncertainties through Equation 8.29 using standard statistical equations.[194] For two uncorrelated variables u, v, with uncertainties σ_u, σ_v, the uncertainty on $x(u,v)$ (σ_x) is calculated as

$$x = au \pm bv,\ \sigma_x = \sqrt{a^2\sigma_u^{\,2} + b^2\sigma_v^{\,2}}\ , \tag{8.41}$$

$$x = \pm auv,\ \sigma_x = x\sqrt{\frac{\sigma_u^{\,2}}{u^2} + \frac{\sigma_v^{\,2}}{v^2}}\ , \tag{8.42}$$

where a and b are constants.

Table 8.7 summarizes the parameters, uncertainties, and correction factors used for calculating k_{isom}/k_{O2}. We obtain $X_{kin} \times X_{prompt}$ of 0.93 ± 0.03 for *n*-butoxy and 0.87 ± 0.04 for 2-pentoxy. Using these correction factors and their uncertainties, **we report k_{isom}/k_{O2} as (1.69 ± 0.15) × 10^{19} cm^{-3} for *n*-butoxy and (3.37 ± 0.43) × 10^{19} cm^{-3} for 2-pentoxy.**

Table 8.7. Parameters, correction factors, 2σ uncertainties, and derived k_{isom}/k_{O2} for *n*-butoxy and 2-pentoxy

		n-butoxy		2-pentoxy	
	Units	Best Value	Uncertainty (2σ)	Best Value	Uncertainty (2σ)
$\left[\left(\frac{\partial\left(\frac{A_0}{A}\right)}{\partial[O_2]}\right)_{[O_2]=0}\right]^{-1}$	10^{19} cm^{-3}	1.81	0.15	3.86	0.45
k_{decomp}/k_{isom}		0.0024	0.0017	0.0648	0.0464
$k_{NO}[NO]/k_{isom}$		0.0262	0.0187	0.0215	0.0154
ϕ_{pi}		0.038	0.018	0.049	0.024
X_{kin}		0.97	0.02	0.92	0.04
X_{prompt}		0.96	0.02	0.95	0.02
$X_{kin} \times X_{prompt}$		0.93	0.03	0.87	0.04
k_{isom}/k_{O2}	10^{19} cm^{-3}	1.69	0.15	3.37	0.43

With the parameters, correction factors, and k_{isom}/k_{O2} calculated for each system, we can compare how well Equation 8.31 (simple linear equation) and Equation 8.29 (full dependence of A_0/A on $[O_2]$) fit to our relative kinetics data. Figure 8.5 compares four different fits to the *n*-butoxy and 2-pentoxy data: the simple linear fit using only the derivative $\left[\left(\frac{\partial\left(\frac{A_0}{A}\right)}{\partial[O_2]}\right)_{[O_2]=0}\right]^{-1}$ (Equation 8.31), and the full dependence (Equation 8.29)

for three different values of ϕ_{pi}: 0%, the best value (4% for *n*-butoxy, 5% for 2-pentoxy), and 20%. These values were chosen to illustrate the extent to which prompt isomerization will cause nonlinearity in the relative kinetics plots.

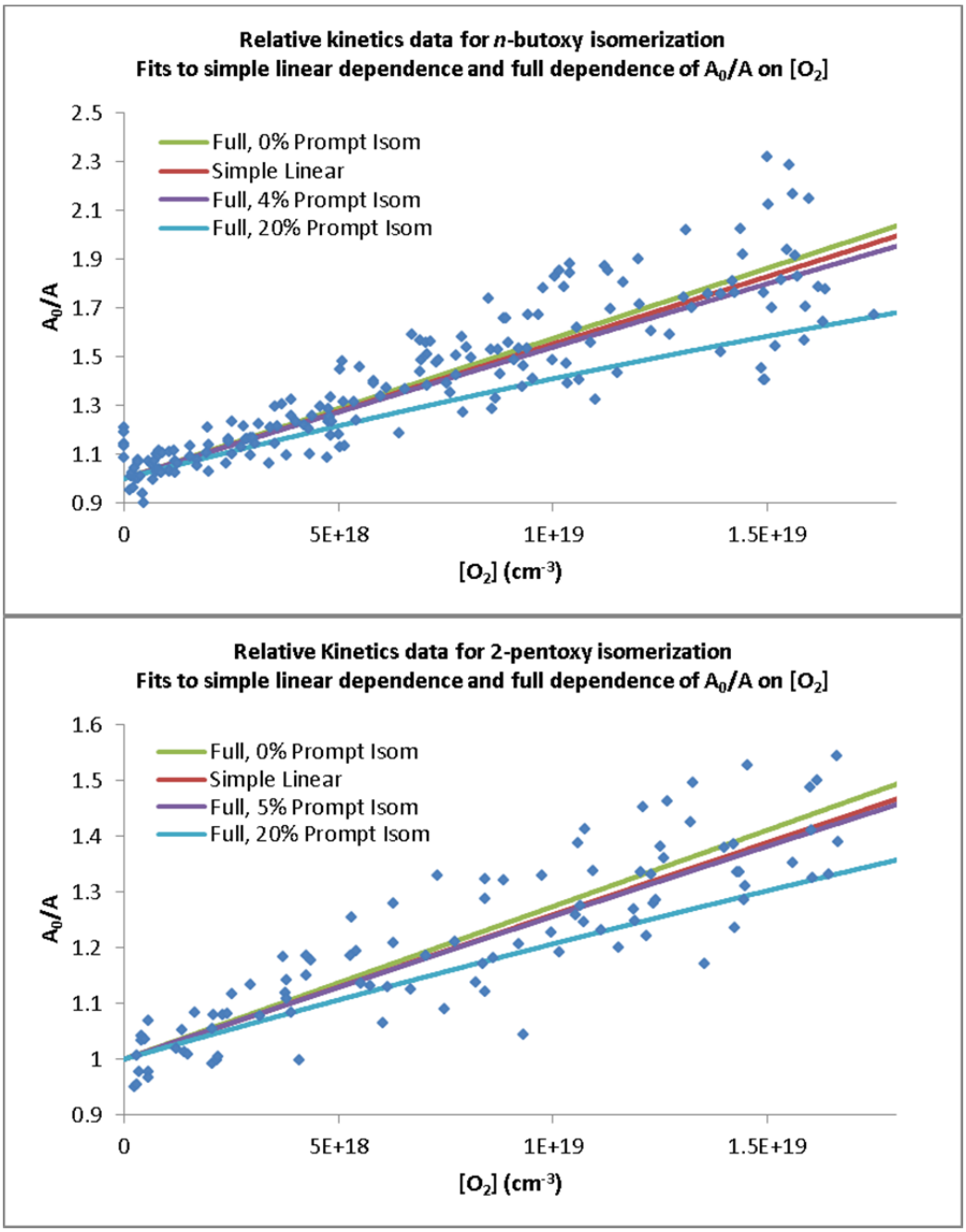

Figure 8.5. Fits of the functional forms of A_0/A vs $[O_2]$ to our CRDS relative kinetics for isomerization of *n*-butoxy (top) and 2-pentoxy (bottom). The simple linear fits (assuming only isomerization and reaction with O_2 are important, Equation 8.31 in the main text) are shown in red. The fits to the full form of A_0/A vs $[O_2]$ (Equation 8.29 in the main text) are

shown for 0% prompt isomerization (green), the best values of prompt isomerization (purple), and 20% prompt isomerization (blue). Adapted with permission from Sprague et al.[31] Copyright 2012 American Chemical Society.

There are two key features of the fits presented in Figure 8.5. First, the simple linear fit and the full fits using the best value of prompt isomerization are in very good agreement across the entire range of $[O_2]$. This result is to be expected; the slopes of both lines at $[O_2] = 0$ are the same, and the relatively small fraction of prompt isomerization causes a small amount of nonlinearity. Second, large values of prompt isomerization (blue curves, ϕ_{pi}=20%) cause too much nonlinearity to model our CRDS data well. This supports our estimates of only 4%–5% of the alkoxy radicals undergoing prompt isomerization.

Discussion

With the new gas concentrations, photolysis ratios, and A_0/A vs $[O_2]$ data, we can readdress three points of interest: comparison of our relative rate k_{isom}/k_{O2} to the values in the literature, the sensitivity of our correction factors to the rate constants and parameters used, and the nature of the products being detected 110 μs after formation of the alkoxy radicals (the time at which our CRDS measurements were made).

Comparison of k_{isom}/k_{O2} Values to the Literature

Table 8.8 contains a comparison of our reanalyzed k_{isom}/k_{O2} values for *n*-butoxy and 2-pentoxy to the rest of the chemical literature (in essence, an updated version of Table 8.1). Our reanalyzed value of k_{isom}/k_{O2} for *n*-butoxy, $(1.69 \pm 0.15) \times 10^{19}$ cm^{-3}, fall on the lower end of the literature values (1.9×10^{19} cm^{-3}), while the initial analysis

(2.3 [+0.2, −0.3] × 10^{19} cm^{-3}) fell at the upper end of the previously reported uncertainties. Our CRDS measurement has lower uncertainty on k_{isom}/k_{O2} (8%, 2σ) than any of the other measured values (minimum of 20%, 2σ) because we can directly detect the primary products of isomerization (HOR•, HOROO•), and their immediate secondary products (shown in Chapter 7 to be HORO•, HOROOH, HOROH, HORROH, and HOR'CHO). Previous experimental studies of the *n*-butoxy radical at 1 atm have obtained values for k_{isom}/k_{O2} ranging from 1.5 × 10^{19} to 2.1 × 10^{19} cm^{-3}.[148, 154-156, 159, 160] The IUPAC data evaluation reports a preferred value of (2.1 ± 1.8) × 10^{19} for k_{isom}/k_{O2} at 298 K and 1 bar pressure, assuming k_{O2} of (1.4 ± 0.7) × 10^{-14} cm^3 $molecule^{-1}$ s^{-1}.[118] The majority of these studies[28, 148, 154, 156, 159, 160] relied on detection of *n*-butanal (the product of alkoxy reaction with O_2) with no detection of the isomerization pathway. Cassanelli et al.[155] quantify the isomerization pathway by measuring 4-hydroxy butanal, a secondary product generated from further reaction of δ-HOC_4H_8OO•. These secondary product analyses are in good agreement with our measured k_{isom}/k_{O2} for *n*-butoxy of (1.69 ± 0.15) × 10^{19} cm^{-3} via direct detection of the isomerization product. This suggests that the secondary chemistry used in previous studies is well modeled, or that the errors in each secondary step cancel each other out. The results of the fast flow study by Hein,[159] which measured NO_2 in real time, were performed at lower pressures (38 torr) and cannot be compared directly to our results. Similarly, our measured k_{isom}/k_{O2} for 2-pentoxy of (3.37 ± 0.43) × 10^{19} cm^{-3} is in good agreement with Atkinson's previous measurements (3.1 × 10^{19} cm^{-3}, factor of 2 uncertainty).[145] Both our and Atkinson's k_{isom}/k_{O2} disagree with Dóbé's result by a factor of 20 (k_{isom}/k_{O2} = 0.15 × 10^{19} cm^{-3}, uncertainty not reported).[157] Dóbé's study used methyl radicals to convert the δ-HO-1-C_5H_{10}• to

2-hexanol, and it is possible that additional secondary chemistry could significantly alter their results.

Our reanalyzed value of k_{isom}/k_{O2} for 2-pentoxy is now higher than the value obtained from the initial analysis, and larger than Atkinson's best value. However, Atkinson's value of k_{isom}/k_{O2} has a large uncertainty (reported as a factor of 2), so our reanalyzed value still comfortably agrees with the only literature value available while having a far lower uncertainty.

Table 8.8. Comparison of relative rate constant determinations k_{isom}/k_{O2} and derived k_{isom} for *n*-butoxy and 2-pentoxy using our reanalysis of Mollner's CRDS data

	k_{isom}/k_{O2} **(10^{19} cm^{-3})**[a]	k_{isom} (10^5 s^{-1})[b]	Molecules detected	Method	*P (torr)*	Ref
***n*-butoxy**	**1.69 ± 0.15**	**2.4 ± 1.2**	**δ-hydroxy-*n*-butyl peroxy**	**Slow flow, CRDS (OH Str)**	**670**	**This work**
	1.96 ± 0.25	2.7 ± 1.4	δ-hydroxy-*n*-butyl peroxy	Slow flow, CRDS (OH Str)	330	Chapter 7
	1.39 ± 0.47	2.0 ± 1.2	δ-hydroxy-*n*-butyl peroxy	Slow flow, CRDS (A-X)	330	Chapter 10
	2.0 ± 0.4	2.7 ± 1.5	Butyl nitrite, Butanal,	Static, FTIR	700	Cassanelli[155]
	1.5 ± 0.4	2.1 ± 1.2	4-hydroxy butanal	Static, GC	760	Cox[156]
	1.9 ± 0.4	2.7 ± 1.4	Butane, Butanal	Static, FTIR	700	Niki[148]
	2.1 ± 0.5	2.9 ± 1.6	Butyl nitrite, Butanal	Slow flow, GC	760	Cassanelli[160]
	1.8 ± 1.1	2.5 ± 2.0	Butyl nitrite, Butanal	Slow flow, GC	760	Cassanelli[160]
	1.8 ± 0.6	2.5 ± 1.5	Butane, Butanal	Static, FTIR	760	Geiger[161]
	0.25 ± 0.19[c]	0.35 ± 0.20[c]	Butanal, 4-hydroxy butanal	Fast flow, LIF	38	Hein[159]
	1.6	2.2	OH and NO_2	Static, GC	740	Carter[154]
	2.1 ± 1.8[d]	2.9 ± 1.4[d]		Recommendation	760	IUPAC[118]
2-pentoxy	**3.37 ± 0.43[e]**	**2.7**	**δ-hydroxy-*n*-pentyl peroxy**	**Slow flow, CRDS (OH Str)**	**670**	**This work**
	3.78 ± 1.62	3.0	δ-hydroxy-*n*-pentyl peroxy	Slow flow, CRDS (OH Str)	330	Chapter 7
	3.1[e]	2.5[e]	2-pentanone	Static, GC	700	Atkinson[145]
	0.15	0.12[f]	Acetone, Acetaldehyde, 2-hexanol	Static, GC	760	Dóbé[157]

a) All uncertainties are 2σ. All studies other than the current work treat all alkoxy reactions besides isomerization and reaction with O_2 as negligible.
b) Computed k_{isom} assuming literature value of $k_{O2} = (1.4 \pm 0.7) \times 10^{-14}$ cm^3 molec^{-1} s^{-1} for *n*-butoxy,[28] and $k_{O2} = 8 \times 10^{-15}$ cm^3 molec^{-1} s^{-1} for 2-pentoxy (no estimate available for the uncertainty).[142]
c) Unlike the other studies, Hein directly measured k_{isom}. In this table, we calculate the ratio k_{isom}/k_{O2} from Hein's measurement using the literature value of k_{O2}.
d) The IUPAC recommendation for k_{isom}/k_{O2} is computed from their individual recommendations of the isomerization and O_2 reactions
e) The uncertainty on k_{isom}/k_{O2} is reported by Atkinson as a factor of 2.
f) Dóbé's study calculates k_{isom} from the relative rate k_{isom}/k_{decomp} and their measured rate $k_{decomp} = 1.2 \times 10^4$ s^{-1}. The k_{isom}/k_{O2} reported in this table uses the literature value of $k_{O2} = 8 \times 10^{-15}$ cm^3 s^{-1} for 2-pentoxy.[142]

While there is good agreement between our k_{isom}/k_{O2} values with the existing literature values, it should be noted that previous studies did not consider how additional alkoxy reactions (decomposition, recombination with NO, prompt isomerization) would affect the calculated value of k_{isom}/k_{O2}. In our experiment, the difference between including and ignoring these three reactions is a factor of $X_{kin} \times X_{prompt}$ (0.93 ± 0.03 for

n-butoxy and 0.87 ± 0.04 for 2-pentoxy). Ignoring these corrections would cause us to systematically overestimate k_{isom}/k_{O2} (by 7% for *n*-butoxy or 13% for 2-pentoxy). It may be necessary to apply similar correction factors to the previous alkoxy relative kinetics experiments. For example, some of the previous *n*-butoxy experiments made use of elevated [NO], as high as 9×10^{14} molec cm^{-3} in order to drive secondary chemistry to completion.[155] For this [NO], the relative rate of reaction with NO to isomerization is $\frac{k_{NO}[\mathrm{NO}\bullet]}{k_{isom}} = 0.12$, roughly equal to the 1σ uncertainties on the previously reported k_{isom}/k_{O2} values. It would be worthwhile to determine whether the previously reported k_{isom}/k_{O2} values for *n*-butoxy require revision in light of the correction factors $X_{kin} \times X_{prompt}$.

The reported correction factors and contributions are valid for our experimental conditions, [NO] = 2×10^{14} molec cm^{-3}; changing [NO] will change the importance of the NO recombination reaction on the relative kinetics analysis. For example, if [NO] = 9×10^{14} molec cm^{-3}, alkoxy recombination with NO becomes very important compared to isomerization ($k_{NO}[NO]/k_{isom} = 0.12$). The change in [NO] from 2×10^{14} molec cm^{-3} to 9×10^{14} molec cm^{-3} will cause a significant change in X_{kin}, from 0.97 to 0.89. A separate correction factor X_{kin} must be computed for each of the previous studies due to the differing [NO] in each experiment.

Sensitivity of Correction Factors to Parameters

The parameters in Table 8.7 show that the major contributions to the correction factors are different for *n*-butoxy and 2-pentoxy. For *n*-butoxy, X_{kin} and X_{prompt} are roughly equal (0.97 and 0.96 respectively). The major contribution to X_{kin} is

recombination with NO ($\frac{k_{NO}[\mathrm{NO}]}{k_{isom}} = 0.026$), while the effects of decomposition are negligible ($\frac{k_{decomp}}{k_{isom}} = 0.002$). In contrast, for 2-pentoxy, X_{kin} is a more significant correction than X_{prompt} (0.92 compared to 0.95). Decomposition is the major contributor to X_{kin} ($\frac{k_{decomp}}{k_{isom}} = 0.065$), although recombination with NO still remains significant ($\frac{k_{NO}[\mathrm{NO}]}{k_{isom}} = 0.022$). The reported correction factors and contributions are valid for our experimental conditions, [NO] = 2×10^{14} molec cm^{-3}; changing [NO] will change the importance of the NO recombination reaction on the relative kinetics analysis.

The parameters within Table 8.7 are subject to somewhat large uncertainties. k_{decomp} is taken as the midpoint of aggregate kinetics experimental data,[117] while k_{NO} is taken from a single experimental study.[32] k_{isom} must be calculated from preliminary values of $k_{\mathrm{isom}}/k_{\mathrm{O2}}$ (discussed above as possibly being too large) and the value of k_{O2} in the literature, determined from a single experimental study.[28] It is instructive to see how the correction factors X_{kin} and X_{prompt}, and therefore $k_{\mathrm{isom}}/k_{\mathrm{O2}}$, vary as a function of each parameter.

Table 8.9 contains the partial derivatives of the correction factors with respect to each parameter at the optimal parameter values (found in Table 8.7). Figure 8.6 shows how the correction factors X_{kin}, X_{prompt}, and $X = X_{\mathrm{kin}} \times X_{\mathrm{prompt}}$ vary with respect to $k_{\mathrm{decomp}}/k_{\mathrm{isom}}$, $k_{\mathrm{NO}}[\mathrm{NO}]/k_{\mathrm{isom}}$, and ϕ_{pi}, for both *n*-butoxy and 2-pentoxy. The derivatives of X with respect to the rate constant parameters are −0.944 for *n*-butoxy and −0.845 for 2-pentoxy. For both systems, the derivatives of X with respect to ϕ_{pi} are approximately 1.

Table 8.9. Sensitivity of Correction Factors X_{kin}, X_{prompt}, and X to parameters k_{decomp}/k_{isom}, $k_{NO}[NO]/k_{isom}$, and ϕ_{pi}

	n-butoxy			2-pentoxy		
	X_{kin}	X_{prompt}	X	X_{kin}	X_{prompt}	X
$\frac{\partial X}{\partial\left(\frac{k_{decomp}}{k_{isom}}\right)}$	−0.945	−0.036	−0.944	−0.847	−0.046	−0.845
$\frac{\partial X}{\partial\left(\frac{k_{NO}[\mathrm{NO}]}{k_{isom}}\right)}$	−0.945	−0.036	−0.944	−0.847	−0.046	−0.845
$\frac{\partial X}{\partial \phi_{pi}}$	0	−1.026	−0.998	0	−1.077	−0.992

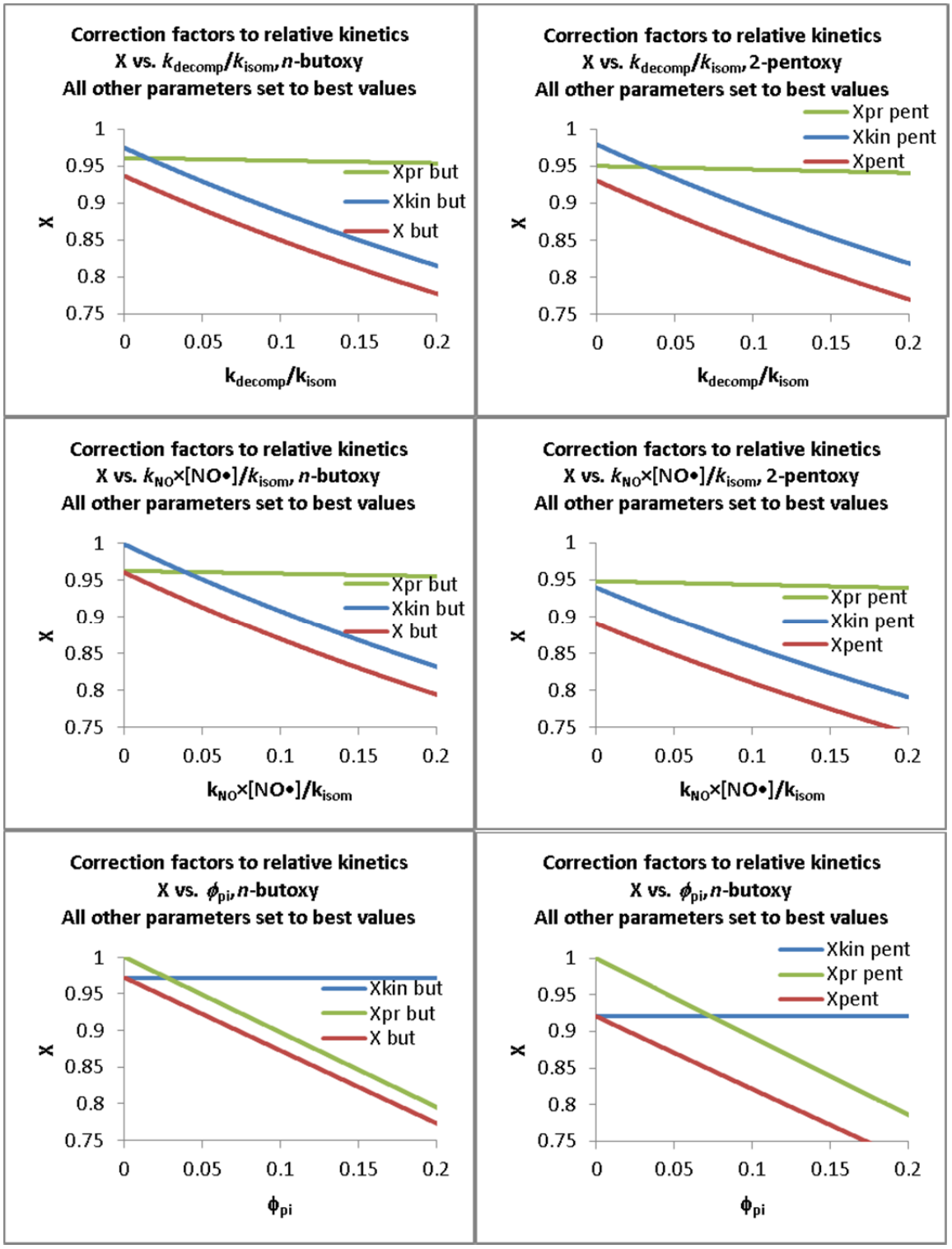

Figure 8.6. Variation of the correction factors X_{kin}, X_{prompt}, and X with respect to the parameters k_{decomp}/k_{isom} (top), $k_{NO}\times[NO]/k_{isom}$ (middle), and ϕ_{pi} (right), for *n*-butoxy (left) and 2-pentoxy (right). The correction factors are defined in the main text. For each plot, the remaining parameters are held constant at their best values, defined in the main text.

Large changes in any of the parameters will cause large changes in *X*. Of particular note are changes in k_{decomp}/k_{isom} for 2-pentoxy (due to the scatter in values calculated from theoretical studies)[117] and changes in $k_{NO}\times[NO]/k_{isom}$ (due to variances in [NO] in the experiments found in the literature).[28, 148, 154, 156, 159, 160] If we compare k_{decomp} = 1×10^4 s^{-1} to 3×10^4 s^{-1} for 2-pentoxy (a factor of 3 difference), k_{decomp}/k_{isom} changes from 0.032 to 0.097. The resulting change in *X* is −0.055, significant with respect to the 2σ uncertainty of 0.05. A change in [NO] from 2×10^{14} molec cm^{-3} to 4×10^{14} molec cm^{-3} (a factor of 2 increase in [NO]) changes $k_{NO}[NO]/k_{isom}$ from 0.026 to 0.052 (*n*-butoxy). This corresponds to a change in *X* of −0.037, significant compared to the reported 2σ uncertainty on *X* of 0.03. The range of [NO] in the literature is much larger than the example presented here, with some experiments using [NO] = 1×10^{15} molec cm^{-3}.[155, 160] It is therefore not possible to define a single, approximate, correction factor that can be used across multiple alkoxy experiments to quickly reanalyze previous studies. Rather, each study must be treated separately with respect to experimental conditions to derive accurate correction factors.

Products Being Detected at 110 μs

In theory, one of the advantages to studying alkoxy isomerization using cavity ringdown spectroscopy is the ability to detect the primary products of isomerization: HOR• (and its dimer HORROH) and HOROO•. As observed in Chapter 7, significant secondary chemistry occurs in the first 110 μs after formation of the alkoxy radicals, the point at which the relative kinetics data collected by Mollner[30] and presented in this chapter were measured. **Therefore, we cannot claim that the relative kinetics that we**

measured in this chapter's OH stretch experiment are solely due to the primary products of isomerization. However, the direct kinetics measurements (Chapter 7) of the OH stretch peaks for both alkoxy isomerizations (*n*-C_4H_9O• and 2-$C_5H_{11}O$•) show that the OH stretch intensity remains constant for at least 800 μs, indicating that regardless of secondary chemistry, the ν_1 band is a good measure of the isomerization pathway. These ideas give us confidence that **our reported k_{isom}/k_{O2} values are still valid, despite the fact that a significant fraction of the measured products were actually secondary products.** Computed intensities and modeled relative kinetics data are discussed in Chapter 9 to support the idea that secondary reactions will not affect the relative kinetics experiment.

To determine the products being detected 110 μs after alkoxy generation, we use the same kinetics models that were used to analyze the spectroscopy experiment in Chapter 7. The model is described in detail in Chapter 9, here we only cite the results of the modeling. Rate constants used in the model were taken directly from the JPL Data Evaluation, NIST Kinetics Database, or the IUPAC Gas Kinetic Data Evaluation.[27, 117, 118] For reactions where no kinetic information was available, best estimates were made from analogous reactions within the databases. All modeling was performed using the Kintecus 3.95 software. [191]

A separate model for 2-pentoxy was not created, given the lack of available rate constants and the added complexity due to the presence of an extra carbon. While the exact nature of the secondary products will differ between the *n*-butoxy and 2-pentoxy systems, it is expected that the relative concentrations of primary to secondary products should remain roughly the same.

Figure 8.7 shows the –OH containing products over the first 110 μs after $C_4H_9O•$ formation for one set of typical experimental conditions used in the OH stretch experiment ([C_4H_9ONO] = 2.0×10^{16} molec cm^{-3}, [$C_4H_9O•$] = 2.0×10^{14} molec cm^{-3}, [NO] = 2.0×10^{14} molec cm^{-3}, p = 670 torr) for [O_2] = 0 (bath gas N_2) and [O_2] = 2.2×10^{19} molec cm^{-3}.

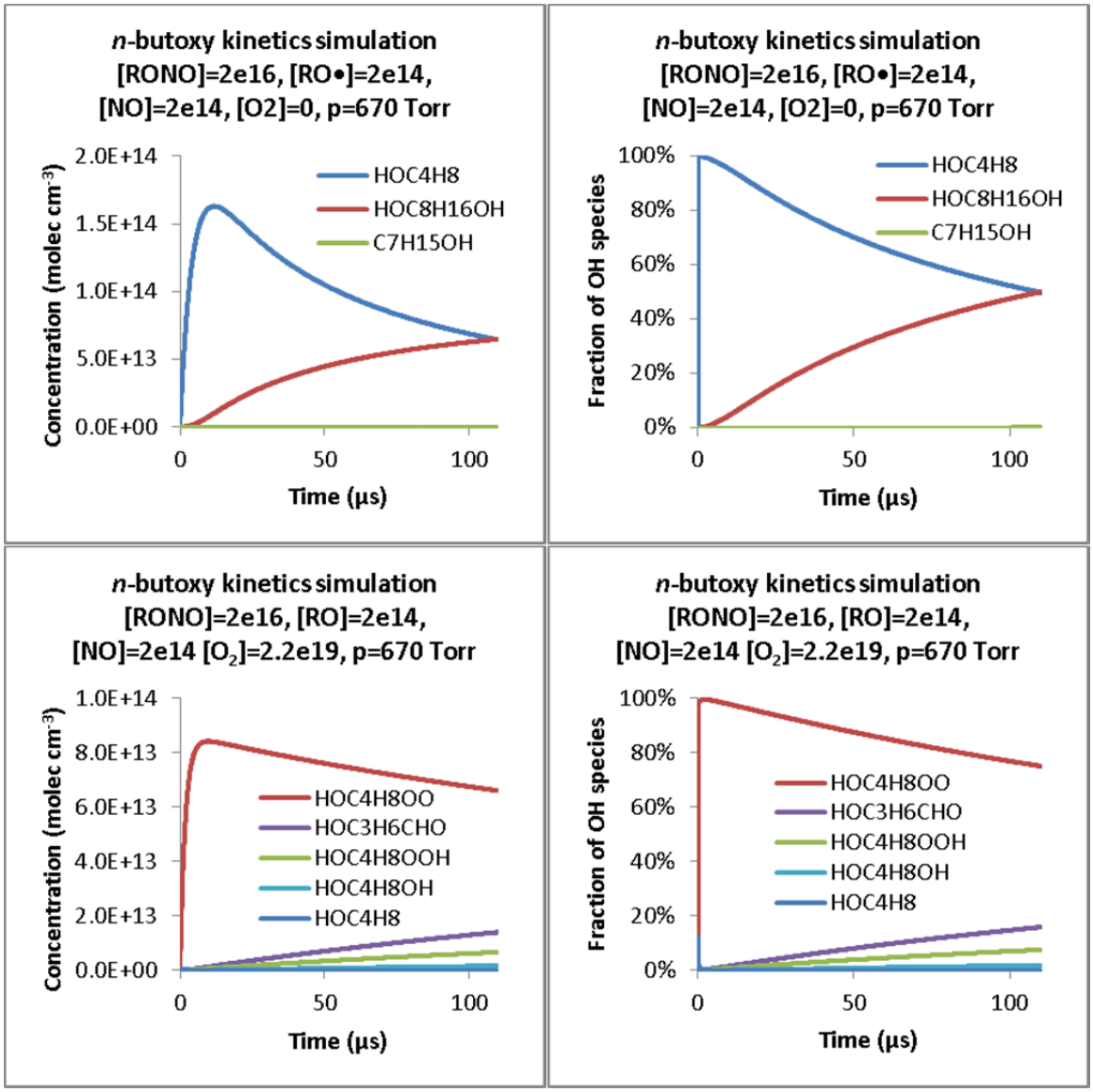

Figure 8.7. Kinetics model of the chemical species contributing to the OH stretch peak in the *n*-butoxy isomerization experiment, for $[O_2] = 0$ (top) and $[O_2] = 2.2 \times 10^{19}$ molec cm^{-3} (bottom), at p = 670 torr, 298 K. The left panels show absolute concentrations, while the right panels show the fraction of total OH molecules that each chemical species makes up. In the absence of O_2, the main products being detected at 110 µs are the direct isomerization product HOC_4H_8• (50%) and its dimer, $HOC_8H_{16}OH$ (50%). For 670 torr of O_2, the main products being detected are the direct isomerization product with O_2 association, HOC_4H_8OO• (75%), and three end-products: HOC_3H_6CHO (16%), HOC_4H_8OOH (7%), and HOC_4H_8OH (2%). Simulations run for $[RONO] = 2 \times 10^{16}$ molec cm^{-3}, $[RO•] = 2 \times 10^{14}$ molec cm^{-3}, and $[NO] = 2 \times 10^{14}$ molec cm^{-3}.

Significant secondary chemistry has taken place 110 μs after formation of the initial C_4H_9O• radicals. In the absence of O_2, only 50% of the OH stretch peak being detected is due to HOC_4H_8•. The remaining isomerization product has dimerized into $HOC_8H_{16}OH$. A very small fraction (0.06%) exists as $C_7H_{15}OH$, formed from the reaction of HOC_4H_8• with the decomposition product C_3H_7•.

In the presence of [O_2], the nature of the products being detected changes. For [O_2] = 2.2×10^{19} molec cm^{-3} (670 torr of O_2, shown in Figure 8.7), four major products contribute to the OH stretch peak. Only 75% of this contribution is due to the primary isomerization product HOC_4H_8OO•. The remainder of the OH stretch intensity comes from stable end-products of the isomerization reaction pathways: HOC_3H_6CHO (16%), HOC_4H_8OOH (7%), and HOC_4H_8OH (2%). It should be noted that previous experiments by Cassanelli et al.[155, 160] used FTIR detection of HOC_3H_6CHO to measure k_{isom}/k_{O2}. Our kinetics model agrees with their experiment: at very long times (10 ms after C_4H_9O• formation), nearly all of the isomerization product has been converted to HOC_3H_6CHO.

The effects of secondary chemistry can be minimized by detecting the isomerization products at an earlier time following generation of the alkoxy radicals, and reducing the absolute radical concentrations used. For example, for the [O_2] = 2.2×10^{19} molec cm^{-3} simulation in Figure 8.7, 97% of the products being detected are HOC_4H_8OO• at 20 μs (as opposed to only 75% at 110 μs). Running the experiment at earlier times would allow for clean spectra of HOC_4H_8• or HOC_4H_8OO• to be obtained. However, care must be taken not to measure the ν_1 band before it has grown in completely (20 μs), as shown in Chapter 7. We have also observed in Chapter 7 that

reducing [RO•] by a factor of 2 leads to even cleaner spectra at 20 μs: >98% $HOC_4H_8OO•$ as opposed to 97%.

Conclusions

Reanalysis of the *n*-butoxy and 2-pentoxy isomerization data sets (OH stretch CRDS experiment) have led to a drastic revision to k_{isom}/k_{O2}, due to previous errors in calculations of $[O_2]$, [RONO], photolysis flux, and data scaling. Furthermore, the effects of additional alkoxy reactions have been shown to be non-negligible, and have now been accounted for. After reanalysis, the k_{isom}/k_{O2} value for *n*-butoxy, $(1.69 \pm 0.15) \times 10^{19}$ cm^{-3} (−26% revision), is in much better agreement with the rest of the chemical literature. Our value for 2-pentoxy, $(3.37 \pm 0.43) \times 10^{19}$ cm^{-3} (+3% revision), has considerably less uncertainty than the only other value in the literature. We have also re-evaluated the amount of prompt isomerization that occurs following photolysis of the alkyl nitrites, and show that a significant amount of the alkoxy radicals do undergo prompt isomerization (4% for *n*-butoxy, 5 % for 2-pentoxy). Because the previous relative kinetics data were taken 110 μs after photolysis, a mixture of primary and secondary products were detected in the OH stretch experiments. In the absence of O_2, the major products being detected were the primary isomerization product $HOC_4H_8•$ (50%), and its dimer $HOC_8H_{16}OH$ (50%). In the presence of 670 torr of O_2, the major products being detected were the primary isomerization product $HOC_4H_8OO•$ (75%) and three end-products: HOC_3H_6CHO (16%), HOC_4H_8OOH (7%), and HOC_4H_8OH (2%).

The alkoxy studies reported in the literature do not consider reactions besides isomerization and reaction with O_2. It is currently unknown to what extent these previous

studies are affected by other alkoxy reaction pathways. It is possible that the correction factors reported in this chapter must be applied to the previously reported k_{isom}/k_{O2}, although this idea has not yet been explored.

Acknowledgements

We thank Andrew K. Mollner for his work on the initial alkoxy relative kinetics experiments. The experiments and reanalysis performed in this chapter were funded under NASA Upper Atmosphere Research Program Grants NAG5-11657, NNG06GD88G, and NNX09AE21G2, California Air Resources Board Contract 03-333 and 07-730, National Science Foundation CHE-0515627, and a Department of Defense National Defense Science and Engineering Graduate Fellowship (NDSEG).